VOL. 1 Nº 1 1978

Instituto de Física Universidad Nacional Autónoma de México

# NOTAS DE FISICA

## The Nuclear Field Theory

D.R. Bes

# notas de física

## the nuclear field theory

d. bes

# THE NUCLEAR FIELD THEORY

Daniel R. Bes*
Departamento de Física
Comisión Nacional de Energía Atómica
Buenos Aires
Argentina

Lectures given at the Escuela Latinoamericana de Física
Mexico, August 1977

---

*Fellow of the CONICET, Argentina

In the study of the nuclear spectrum, we are faced with the problem of fermions moving in a set of single-particle levels and interacting through a residual force. There are several methods to treat this problem:

i) Perturbation theory. One uses the independent-particle Hamiltonian as unperturbed Hamiltonian. However, a typical matrix element of the residual interaction turns out to be of the same order of magnitude as the distance between the single-particle levels within a major nuclear shell (O(1 MeV)). Therefore, a straight forward perturbation theory cannot be expected to converge. An empirical verification of this statement is found, for instance, in the fact that the binding energies of even even nuclei do not show discontinuities within a major shell, thus indicating that the different configurations are completely mixed (Wa 71).

ii) Shell model diagonalizations. Within this framework, important theoretical results have been obtained in the neighborhood of closed shells. A description of modern shell model calculations is found in (Wi 77). Although this approach is relatively clear from the conceptual point of view, it presents computational difficulties even in light nuclei, where the shell degeneracies are smaller. For instance, calculations in the $16 < A < 40$ region require the $p_{1/2}$, $d_{5/2}$ and $s_{1/2}$ single-particle levels at the beginning of the shell, and the $d_{5/2}$, $s_{1/2}$ and $d_{3/2}$ levels at the end. A calculation using the four single-particle levels is not yet available.

iii) Elementary modes of excitation. The aim of this method is to express the complicated spectra in terms of relatively few building blocks. These include not only single-particle excitations, but also different collective (boson) excitations. Objections to this approach are that the basic set of states violates the Pauli principle and is overcomplete (since the independent particle degree of freedom exhausts all the degrees of freedom which are present in the problem). Furthermore, one has no apriori knowledge about the interaction between the elementary modes.

In these series of lectures we develope in detail a method which allows to eliminate the errors inherent to method iii) in a systematic way.

## II. ELEMENTARY MODES OF EXCITATION

They represent a generalization of the concept of the normal modes of vibrations in a classical system. Thus, they provide a basis for expressing the complicated excitations that can be produced in the neighborhood of a given equilibrium configuration. In addition to this practical purpose of economy in expressing the complicated spectra in terms of a relatively few building blocks, the study of the elementary modes is important because the deeper properties of the system are reflected in the nature of these building blocks.

The concept of elementary modes was introduced in Fermi systems by Landau (La 41). Their importance in nuclear physics has been the leit motiv of the Copenhagen School ("The" presentation of this approach is found in (Bo 75)).

The mathematics of the elementary modes is simple. Let us assume that it is possible to recast the many-body Hamiltonian (including a two-body term) as a summation of Hamiltonians $H'_\sigma$ corresponding to separate degrees of freedom,

$$H \rightarrow \sum_\sigma H'_\sigma \qquad (1)$$

with the associated Schroedinger equations

$$H'_\sigma \psi_\sigma(\zeta) = \varepsilon_\sigma \psi_\sigma(\zeta) \qquad (2)$$

Here $\zeta$ represents a generalized variable (e.g. the single-particle coordinate, the gap parameter in a superfluid, the shape of the nucleus, etc.). The wave function $\psi_\sigma(\zeta)$ is the $\zeta$-coordinate representation of the eigenstate $\Gamma^+_\sigma|0\rangle$. The operator $\Gamma^+_\sigma$ creates an excitation with quantum number $\sigma$, when acting on the state $|0\rangle$ (the vacuum of all the excitations $\sigma$).

The energy of the states (or at any rate, of the most important states in order to determine the physical response of the system to external probes) may be of the form

$$E_n = \sum_\sigma n_\sigma \varepsilon_\sigma \qquad (3)$$

while the corresponding eigenstates are

$$|n\rangle = \prod_{\sigma} (n_{\sigma}!)^{-1/2} (\Gamma_{\sigma}^{+})^{n_{\sigma}} |0\rangle \qquad (4)$$

where $n_\sigma = 0$ or 1 in the case of fermions, and $n_\sigma = 0,1,2\ldots$ in the case of bosons.

Additivity features similar to (3) hold for transition matrix elements (e.g. two-particle transfer amplitudes, electromagnetic matrix elements, etc.). For instance, for the operator $A_{op}$ which specifically excites the eigenstates $\psi_\sigma(\zeta)$,

$$\langle n|A|m\rangle = \sum_{\sigma} A_{\sigma} n_{\sigma}^{1/2} \delta(n_{\sigma}, m_{\sigma}+1)$$

$$A_{op} \rightarrow \sum_{\sigma} A_{\sigma} \Gamma_{\sigma}^{+} \qquad (5)$$

where $A_\sigma$ is the matrix element between the states $n_\sigma = 0$ and $n_\sigma = 1$ of the operator $A_{op}$.

Because the excitation energies $E_m$ and transition matrix elements $\langle n|A|m\rangle$ are linear combinations of $\epsilon_\sigma$ and $A_\sigma$ respectively, the eigenstates $\psi_\sigma(\zeta)$ are called elementary excitations of the system.

With the help of experimental probes which couple weakly to the nucleus (i.e. in such a way that the system can be expressed in terms of the properties of the excitation in the absence of probes) it has been possible to identify the elementary modes which are listed in table II-1. Two simple examples will be discussed in the following, rather than a systematic review on each of the modes. "The central theme is the dialetic between classical macroscopic pictures and the microscopic quantal structures that emerge as soon as one expresses those pictures in terms of the motions of neutrons and protons that move in quantized orbits exhibiting shell structure" (Mo 77).

## SURFACE PHONONS

The simplest example of a collective vibrational mode that we can consider is that of a shape oscillation of a nucleus with spherical equilibrium. Small deformations may be described by expanding the surface R in multipoles.

$$R(\theta,\phi) = R_0 \left(1 + \sum_{\lambda,\mu} \alpha_{\lambda\mu} Y^{*}_{\lambda\mu}(\theta,\phi)\right) \qquad (6)$$

For an oscillatory motion the deformation coordinates $\alpha_{\lambda\mu}$ are functions of time. Expanding the density in powers of the deformation, we obtain

$$\rho(r,\alpha) = \rho(r,\alpha=0) + \alpha\frac{d\rho}{d\alpha}$$
$$= \rho_o(r) - R_o\frac{d\rho_o}{dr}\sum_{\lambda\mu}\alpha_{\lambda\mu}\, Y^*_{\lambda\mu}(0\phi) \qquad (7)$$

So far, our language has been purely classical and macroscopic. Such deformation may also be expressed in terms of the excitations of particles in the quantal system. If this system has a predominantly single-particle character, and if the potential has the same shape as the density (7), we must consider a field of the form $F\alpha\frac{d\rho}{dr}Y_{\lambda\mu}$. The collective properties of the quantal system depends on the "single-particle response function", i.e. of the spectrum of excitations produced by the field F. Since the radial $\frac{d\rho}{dr}$ is peaked at the nuclear surface, it is often convenient to use for the one-particle field the multiple moment

$$Q_{\lambda\mu} = i^\lambda r^\lambda Y_{\lambda\mu}(\theta\phi) \qquad (8)$$

An example of a single-particle response function for the field (8) with $\lambda = 3$, given in fig. II-1, shows a tendency towards concentration of strength around $\omega_o$ and $3\omega_o$ (signature of the harmonic oscillator selection rules).

The particle-hole states[+] $|\nu;\lambda\mu\rangle = \gamma^+_{\nu,\lambda\mu}|0\rangle = [a^+_k a_i]^\lambda_\mu|0\rangle$ in fig. II-1 have energies $E_\nu$, matrix elements $q_\nu = \langle\nu,\lambda\mu|Q_{\lambda\mu}|0\rangle$ and are created by the operator $\gamma^+_{\nu,\lambda\mu}$. There are $\Omega \gg 1$ of such configurations. Any superposition of them (like $\gamma^+\gamma^+|0\rangle$) is also a possible state of the system[++]. The independent superposition of excitations is the essential feature characterizing quantal harmonic

---

[+] $\nu = \nu(k,i)$; $\varepsilon_k > \varepsilon_f$ and $\varepsilon_i < \varepsilon_f$

[++] This statement can be justified in the limit of large $\Omega$ because of the fact that there are $\Omega^2$ states of the type $\gamma^+\gamma^+|0\rangle$ out of which only $\Omega$ states should be excluded. Therefore we introduce an error of order $\Omega^{-1}$ by neglecting the Pauli principle.

oscillations. Thus, the creation and annihilation operators $\gamma^+, \gamma$ may be viewed as the one-phonon creation and annhilation operators. They approximately satisfy the conmutation relation $\gamma^+_{\nu,\lambda\mu}\gamma_{\omega,\lambda\mu} - \gamma_{\omega,\lambda\mu}\gamma^+_{\nu,\lambda\mu} = \delta_{\nu\omega}\,\delta_{\lambda\lambda}\,\delta_{\mu\mu}$.

The zero order Hamiltonian (in which the effects of the interaction are not yet included) and the zero order field are approximated by

$$H_\lambda^{(0)} \simeq \sum_{\nu,\mu} E_\nu\, \gamma^+_{\nu,\lambda\mu}\, \gamma_{\nu,\lambda\mu} \quad ; \quad E_\nu = \varepsilon_k - \varepsilon_i$$

$$Q^{(0)}_{\lambda\mu} \simeq \sum_\nu q_\nu \,(\gamma^+_{\nu,\lambda\mu} + (-)^{\lambda-\mu}\gamma_{\nu,\lambda-\mu}) \; ; \; q_\nu = -(2\lambda+1)^{-1/2} \;\langle k\|i^\lambda r^\lambda Y_\lambda\|i\rangle \tag{9}$$

The residual effective interactions produce linear combinations of the unperturbed excitations,

$$\Gamma^+_{n,\lambda\mu} = \sum_\nu (X_{n,\nu}\gamma^+_{\nu,\lambda\mu} - (-)^{\lambda-\mu} Y_{n,\nu}\,\gamma_{\nu,\lambda-\mu}). \tag{10}$$

The new normal modes $\Gamma^+$ are determined by the phonon linearization equation

$$[(H^{(0)} + H_{int}) \;,\; \Gamma^+] \simeq \omega\,\Gamma^+ \tag{11}$$

The solution of (11) becomes specially simple when the force is separable[+].

$$H_{int} = -\frac{1}{2}\,\chi_\lambda \sum_\mu |Q_{\lambda\mu}|^2 \simeq -\frac{1}{2}\chi_\lambda \sum_\mu |Q^{(0)}_{\lambda\mu}|^2 \tag{12}$$

In this case, the phonon energies $\omega_n$ are given by the roots of the dispersion relation

$$\chi_\lambda^{-1} = 2\sum_\nu |q_\nu|^2\, E_\nu/\,(E_\nu^2 - \omega_n)^2 \tag{13}$$

while the amplitudes $X_{n,\nu}$ and $Y_{n,\nu}$ are

$$X_{n,\nu} = -(2\lambda+1)^{1/2}\,\Lambda_n\, q_\nu\,/(E_\nu - \omega_n)$$
$$Y_{n,\nu} = -(2\lambda+1)^{1/2}\,\Lambda_n\, q_\nu\,/(E_\nu + \omega_n) \tag{14}$$

where

$$\Lambda_n = \frac{1}{2}\left(\frac{2\lambda+1}{\omega_n}\right)^{1/2} \left[\sum_\nu |q_\nu|^2 E_\nu\,/(E_\nu^2 - \omega_n^2)^2\right]^{-1/2} \tag{15}$$

---

+ The justification of the use of effective separable forces and the prediction of their strength $\chi_\lambda$ is found in (Bo 75), (Mo 77). For the quadrupole case, see ... (Be 69)

By inverting the transformation (10), it is easy to obtain the matrix elements of the multipole operator $Q_{\lambda\mu}$. In particular, the matrix element between the zero and the one phonon states is

$$\langle \Gamma^{+}_{n,\lambda\mu} | Q_{\lambda\mu} | 0 \rangle \simeq \sum_{\nu} q_{\nu} \, (X_{n,\nu} + Y_{n,\nu}) = -(2\lambda+1)^{1/2} \Lambda_n \chi_\lambda \qquad (16)$$

$$(Q_{\lambda\mu})_{coll} = -(2\lambda+1)^{1/2} \chi_\lambda^{-1} \sum_{n} \Lambda_n \left[ \Gamma^{+}_{n,\lambda\mu} + (-)^{\lambda-\mu} \, \Gamma_{n,\lambda-\mu} \right] \qquad (17)$$

The response function corresponding to the normal modes is given in fig. II-2. There is a very large concentration of strength in a single state lying below $\omega_o$. The 2.62 MeV $3^-$ state in $Pb^{208}$ appears as the one-phonon state of a quantal collective vibrator, which thus is the quantal version of the macroscopic classical oscillation of the liquid drop.

The present method of obtaining quantal vibrators is called the random phase approximation (RPA).

The interpretation of the 2.62 MeV state as the one-phonon state of an octupole oscillator relies on the fact that B(E3)= 39 Bsp >> Bsp, and that $\omega_{3^-}$ = 2.62 MeV < 3.98 MeV (which is the lowest $3^-$ particle-hole excitation) and on some experimental verification of its microscopic structure. However, other descriptions (such as a permanent octupole deformation) could produce similar effects. The experimental determination of the two-phonon quadruplet at 5.2 MeV ($J = 0,2,4,6$) should provide a decisive test on the picture. This challenging experiment is crucial, since too many basic concepts of nuclear structure rely on the interpretation of this $3^-$ state.

| mode | specific excitation mechanism: formalism | experiments |
|---|---|---|
| single-particle motion | $a^+(\nu)$ , $a(\nu)$ | single-particle addition or removal |
| density oscillations | $(a^+a)$ | |
| shape | $\lvert a^+(j)a(j')\rvert^\lambda$ | |
| isospin | $\Sigma(a^+a)_n-(a^+a)_p$ | inelastic scattering |
| spinflip | $(a^+_\uparrow a_\downarrow)$ | |
| others | ..... | |
| pair vibrations | $\lvert a^+(j)a^+(j')\rvert^\lambda$ | two particle transfer |
| nucleonic excitation | | |
| "(33) resonance" | $a^+_\pi a_\pi$ | pion scattering |
| hyper nuclei | $(c^+_\pi c_K)$ | $(K\pi)$ exchange |
| rotations | low frequency vibrational modes that separate out whenever an average field violates one of the symmetries of the total Hamiltonian. | |

Table II-1. Elementary modes of excitation in nuclei (from (Ko 77)).

Figure Captions

Fig. II-1. The single-particle response function for $\lambda=3$ in the nucleus with $Z=46$ and $N=60$ (Bo 75). It has been obtained from a Nilsson potential $V(r) = \hbar\omega_o[\frac{1}{2} m\omega_o r^2 - 0.10\ \ell.s - 0.22(\ell^2 - \langle\ell^2\rangle_N)]$ with $\omega_o = 41\ A^{-1/3}$ MeV.

Fig. II-2. The response function corresponding to the octupole modes in $Pb^{208}$. The calculation has been made using the experimentally known single-proton and single-neutron levels in $Bi^{209}$, $Pb^{209}$, $Tl^{207}$ and $Pb^{207}$. In the upper part, the B(E3) values for exciting particle-hole states are given in single-particle units. Only transitions with an intensity larger than 0.2 are indicated. An effective charge of 1.13e for protons and 0.13e for neutrons has been used in order to take into account polarization effects associated with the $\Delta N=3$ modes (c.f. (Bo 75) and fig. V-3). The lower part of the figure represents the response function for the RPA normal modes. The same renormalized charges have been used. The coupling strengh $\chi_3 = 0.000375\ (m\omega_o)^3$ MeV has been fixed so the lowest $3^-$ state lies at 2.62 MeV. The B(E3) value corresponding to the collective state is 31 $B_{sp}$ in agreement with the experimental value 39 $B_{sp}$ (Zi 68).

For both the upper and lower figure, the energy weighted sum rule is

$$\sum_n \omega_n B(E3,n) = 325\ B_{sp}\ \text{MeV}$$

The normalization constant is $\Lambda_3 = 0.0414\ (m\omega_o)^{3/2}$ MeV.

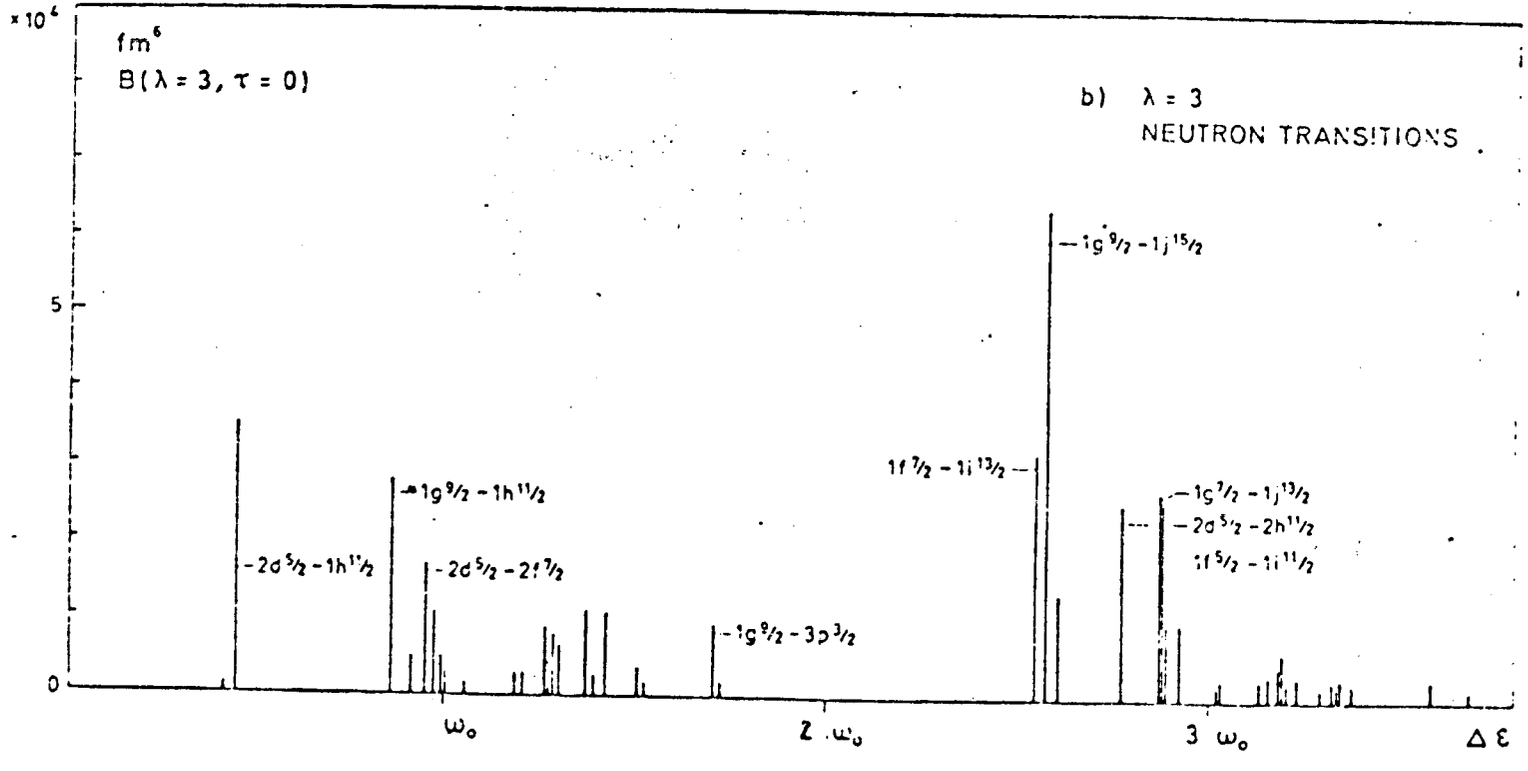
×10⁴
fm⁶
B(λ = 3, τ = 0)
b) λ = 3
NEUTRON TRANSITIONS
5
0
1g9/2 - 1j15/2
1f7/2 - 1i13/2
1g9/2 - 1h11/2
2d5/2 - 1h11/2
2d5/2 - 2f7/2
1g9/2 - 3p3/2
1g7/2 - 1j13/2
2d5/2 - 2h11/2
1f5/2 - 1i11/2
ω₀
2 ω₀
3 ω₀
Δ ε

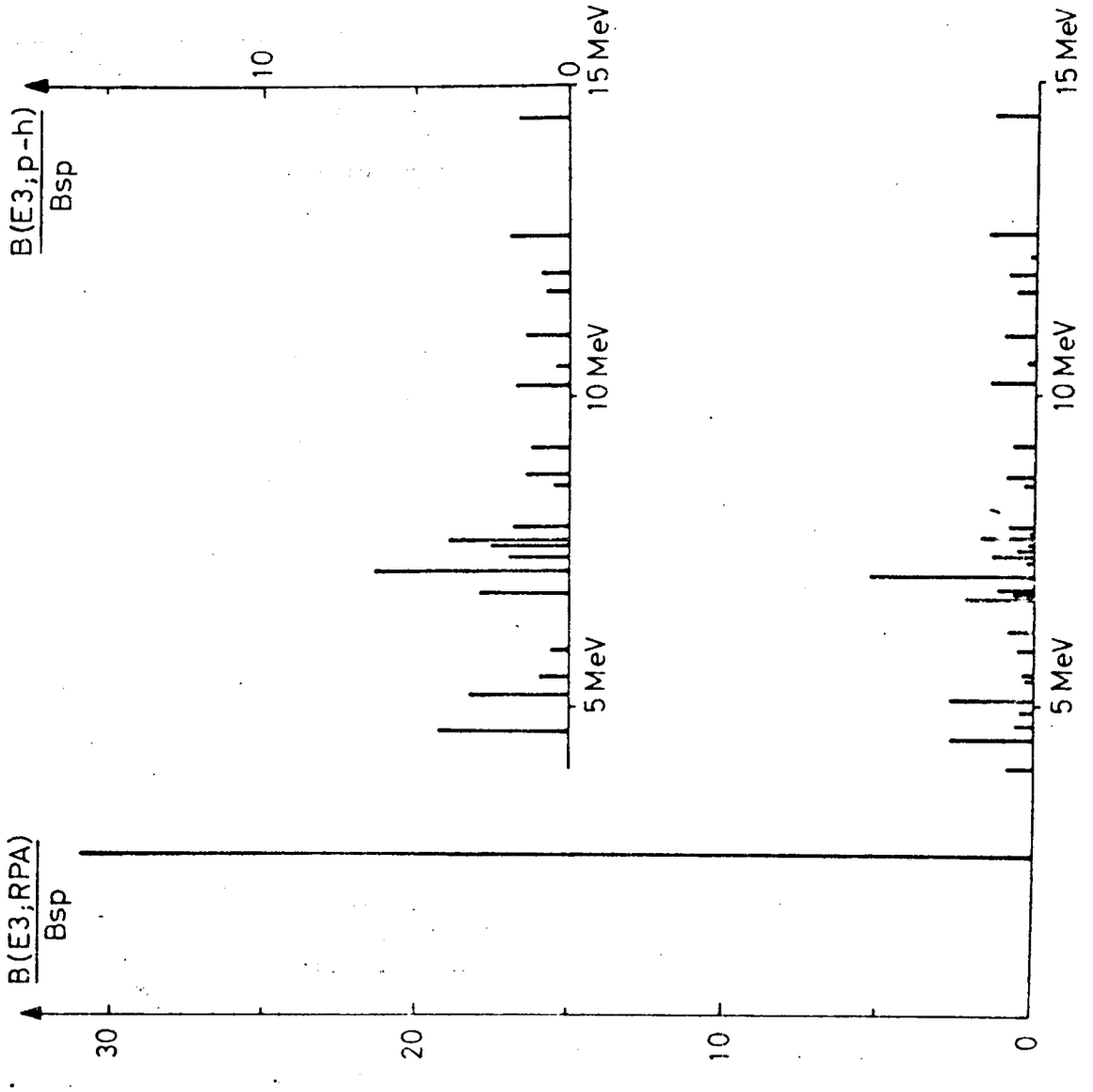
B(E3;RPA)/Bsp
30
20
10
0
5 MeV
10 MeV
15 MeV
B(E3;p-h)/Bsp
10
0
5 MeV
10 MeV
15 MeV

Fig. II-2

## III. PAIRING PHONONS

We saw in the previous section that quantal collective harmonic oscillations of a fermionic system are obtained in the limit that the particle-hole pairs behave as independent phonons. This limit implies large degeneracies $\Omega$.

The coupling of these phonons through appropriate residual interactions yields the normal modes of the system.

Identical procedure can be applied if we consider as unperturbed phonons the addition or removal of pairs of particles. For large degeneracies, the states thus obtained can be considered as one-boson states of corresponding harmonic oscillators. The normal modes of the system are called pairing phonons (Bo 64), (Be 66).

The one-pairing phonon states belong to nuclei with one pair of particles more or less than the ground state (i.e., they carry a different quantum number . The same is true for surface bosons in which the angular momentum plays the same role as the number of particles for pairing phonons).

The equivalent operator to the multipole moment $Q_{\lambda\mu}$ is an operator that creates and destroys two particles. An operator of this type acts in a (direct) two-body transfer reaction, such as (t,p). Indeed, the systematics of two-neutron transfer reactions (Br 73) indicate that the population of the lowest $0^+$ state (ground state) is generally larger by one or two orders of magnitude than the population of excited $0^+$ states. This fact is characteristic of a cooperative effect, in the same way as the strong matrix element to the lowest surface mode associated with each multipolarity indicates strong coherence.

Let us consider for the moment pairing phonons in a closed shell ($Pb^{208}$) carrying zero angular momentum and corresponding to identical particles. The geometrical coupling of these bosons is simple, since the one-phonon state has only two components (addition and removal) and thus they correspond to a two-dimensional harmonic oscillator. The quantum numbers labelling the spectrum

are $(n_r, n_a)$, the number of removal and addition phonons (fig. III-1).

The vacuum state $|(0,0)> = |0>$ represents the ground state[+] of $Pb^{208}$. The one-phonon states are the ground states of $Pb^{206}$ and $Pb^{210}$

$$|Pb^{206}, gs> = |(1,0)> = \Gamma_r^+|0> \qquad (1)$$

$$|Pb^{210}, gs> = |(0,1)> = \Gamma_a^+|0>$$

The cross sections

$$\sigma(Pb^{208}(p,t)\ Pb^{206}) = \sigma((0,0)(p,t)(1,0)) = r$$

$$\sigma(Pb^{208}(t,p)\ Pb^{210}) = \sigma((0,0)(t,p)(0,1)) = a \qquad (2)$$

are the units in which we measure other transitions.

The concept of elementary excitations require that the quanta retain their identity when super imposed to other excitations of the same or different type. There are three states with two pairing phonons, namely (1,1), (0,2) and (2,0).

The state (1,1). The excitation energy of this state in $Pb^{208}$ is predicted to be the sum of the addition and removal phonon energies $\omega_a + \omega_r$

$$\Delta E(1,1) = -B(Pb^{206}) - B(Pb^{210}) + 2B(Pb^{208}) = 4{,}989\ MeV \qquad (3)$$

in excellent agreement with the experimental energy (fig. III-1). Here B is the binding energy (Wa 71). Moreover, the cross sections $\sigma((1,0)(t,p)(1,1)) = (0.91 \pm 0.$ and $\sigma((0,1)(p,t)(1,1)) = (1.27 \pm 0.20)r$ are in agreement with the predicted values a and r, respectively.

The comparison between energies of states with $A \neq 208$ requires the substraction of a linear term in the number of particles, which is alien to the pairing mode. For simplicity, we adjust the factor in the linear term so that $\omega_a = \omega_r$ (= 2.494 MeV); thus one uses

$$E(\pi) = B(Pb^{208}) - B(\pi) + 11.616\ \pi\ MeV \qquad (4)$$

---

+ In this phenomenological approach, it is immaterial whether ground state correlations are included or not.

where $\pi$ is the number of pairs of particles added to the closed shell. Using this correction, the predicted energy of the $|(0,2);\ Pb^{212}(gs)>$ state is only 169 keV below the experimental value, while this discrepancy increases to 706 keV for the $|(2,0);\ Pb^{204}(gs)>$ state†. The cross sections are compatible with the model prediction although somewhat small for the removal case (fig. III-1).

Another characteristic of the harmonic oscillator is the vanishing of transition matrix elements of the coordinate operator between states differing by more than one phonon. The (2,1) (excited) state in $Pb^{206}$ is not populated in the (0,0)(p,t) reaction with an upper limit $< 0.03r$.

There is also good evidence for the validity of the harmonic description for the quadrupole pairing phonons. The one-phonon states are in this case:

$$\begin{aligned} |Pb^{206},\ 803\ \text{keV}> &= \Gamma^{+}_{r,\lambda=2\,\mu}\,|0> \\ |Pb^{210},\ 795\ \text{keV}> &= \Gamma^{+}_{a,2\mu}\,|0> \end{aligned} \qquad (5)$$

Therefore, two almost degenerate $2^+$ states are to be found in $Pb^{208}$, namely

$$|1> = \Gamma^{+}_{r,o}\ \Gamma^{+}_{a,2}\ |0> \ ;\ |2> = \Gamma^{+}_{r,2}\ \Gamma^{+}_{a,o}\ |0> \qquad (6)$$

which have been found at the predicted energy $\simeq 2\omega_{a,o}$ + 800 keV, with an empirical splitting of 95 keV and completely mixed with each other (fig. III-2).

The multipole pairing two-body force is defined by (Be 71), (Bo 77)

$$H_p = -\,G_\lambda\ (2\lambda+1)\ \sum_{\mu}\ P^{+}_{\lambda\mu}\ P_{\lambda\mu} \qquad (7)$$

where

$$P^{+}_{\lambda\mu} = \left(\frac{4\pi}{2\lambda+1}\right)^{1/2}\left[\sum_{\nu}\ p_\nu\ \gamma^{+}_{\nu,\lambda\mu} + (-)^{\lambda-\mu}\ \sum_{\eta}\ p_\eta\ \gamma_{\eta,\lambda\mu}\right] \qquad (8)$$

$$\gamma^{+}_{\nu,\lambda\mu} = \left[a^{+}_{k_1}\,a^{+}_{k_2}\right]^{\lambda}_{\mu}/(1+\delta_{12})^{1/2} \qquad \gamma^{+}_{\eta,\lambda\mu} = -\left[a_{i_1}\,a_{i_2}\right]^{\lambda}_{\mu}/(1+\delta_{12})^{1/2}$$

$$p_\nu = <k_1\|i^\lambda\ Y_{\lambda\mu}\|\,k_2>/(1+\delta_{12})^{1/2} \qquad p_\eta = <i_1\|i^\lambda\ Y_{\lambda\mu}\|i_2>/(1+\delta_{12})^{1/2}$$

---

† These discrepancies are analyzed in section IX.

with $\varepsilon_k > \varepsilon_F, \varepsilon_i < \varepsilon_F$ and $k_1 \geq k_2$, $i_1 \geq i_2$. We denote by $E_\nu(E_\eta)$ the unperturbed energy of a two-particle (two-hole) state. The creation operators for the normal modes are defined

$$\Gamma^+_{an,\lambda\mu} = \sum_\nu X_{n,\nu}\, \gamma^+_{\nu,\lambda\mu} - (-)^{\lambda-\mu} \sum_\eta Y_{n,\eta}\, \gamma_{\eta,\lambda-\mu}$$
$$\Gamma^+_{rn,\lambda\mu} = \sum_\eta X_{n,\eta}\, \gamma^+_{\eta,\lambda\mu} - (-)^{\lambda-\mu} \sum_\nu Y_{n,\nu}\, \gamma_{\nu,\lambda-\mu} \qquad (9)$$

The linearization equations $\left[(H_{sp} + H_p),\ \Gamma^+\right] = \omega\Gamma^+$ yield

$$(4\pi G_\lambda)^{-1} = \sum_\nu |P_\nu|^2/(E_\nu - \omega_{an}) + \sum_\eta |P_\eta|^2/(E_\eta + \omega_{an})$$
$$= \sum_\nu |P_\nu|^2/(E_\nu + \omega_{rn}) + \sum_\eta |P_\eta|^2/(E_\eta - \omega_{rn}) \qquad (10)$$

For reasonable values of $G_\lambda$, imaginary roots are present in most of medium and heavy nuclei. The only exceptions are the closed shell nuclei, where there is a large gap between the levels above and below the Fermi energy. In this case, there are two real roots, namely $\omega_{a1}$ and $\omega_{r2}$ which become sizeably separated from their unperturbed position. For $\lambda=0$, these separations represent the increase in the ground state binding energies due to the pairing force in the nuclei with one pair of particles more or less than the closed shell. The lowest roots ($\lambda=0,2,4,6$) are reproduced around $Pb^{208}$ using $G_\lambda = (27/A \pm 10\%)$ MeV. (Br 74).

The amplitudes X, Y are

$$X_{n,\nu} = \Lambda_{an}\, P_\nu/(E_\nu - \omega_{an}) \qquad Y_{n,\eta} = \Lambda_{an}\, P_\eta/(E_\eta + \omega_{an})$$
$$X_{n,\eta} = \Lambda_{rn}\, P_\eta/(E_\eta - \omega_{rn}) \qquad Y_{n,\nu} = \Lambda_{rn}\, P_\nu/(E_\nu + \omega_{rn}) \qquad (11)$$

where

$$\Lambda_{an} = \left[\sum_\nu |P_\nu|^2/(E_\nu - \omega_{an})^2 - \sum_\eta |P_\eta|^2/(E_\eta + \omega_{an})^2\right]^{-1/2}$$
$$\Lambda_{rn} = \left[-\sum_\nu |P_\nu|^2/(E_\nu + \omega_{rn})^2 + \sum_\eta |P_\eta|^2/(E_\eta - \omega_{rn})^2\right]^{-1/2} \qquad (12)$$

Thus, inverting (9) one obtains

$$(P^{+}_{\lambda\mu})_{coll} = G_{\lambda}^{-1}\left[4\pi(2\lambda+1)\right]^{-1/2} \sum_{n}\left[\Lambda_{an}\Gamma^{+}_{an,\lambda\mu} + (-)^{\lambda-\mu}\,\Lambda_{rn}\Gamma_{rn,\lambda-\mu}\right] \quad (13)$$

The parameters $\Lambda_{an}$ ($\Lambda_{rn}$) are proportional to the two-particle transfer spectroscopic amplitude relating the closed shell nucleus ground state and the two-particle (two-hole state) if the operator responsible for the two-body transfer process the one given by eq. (8). This is not completely true, but it gives a reasonable estimation of the amplitudes. A more refined calculation can be performed by introducing the amplitudes $\langle n|\left[a^{+}_{j}a^{+}_{j'}\right]^{\lambda}|0\rangle$ (which are obtained by inverting (9)) into the direct reaction codes. This calculation has been performed in (Fl 72).

Figure Captions

Fig. III-1. The many-phonon pairing spectrum around $^{208}$Pb (Be 77c). The energies predicted by the pairing vibrational model are displayed as dotted horizontal lines while the experimental values are drawn as continuous lines. The harmonic quantum numbers ($n_r$, $n_a$) are indicated for each level. A schematic representation of the many-particle many-hole structure of the state is also given. The transitions predicted by the model are indicated in units of r and a (eq.(2)). The corresponding experimental numbers are also given together with their errors above each level. The dotted line between the states (0,0) and (2,1) indicates that the $^{208}$Pb(p,t)$^{206}$Pb reaction to the three-phonon states in $^{206}$Pb was carried out and an upper limit of 0.03 r for the corresponding cross section was determined. The (p,t) data is from (La 73) and the (t,p) data from (El 71), (Fl 72a), (Fl 72b), (Fl 74) and (Ig 71).

Fig. III-2. The pairing vibrational model for the $J^{\pi} = 0^+$ and $2^+$ excited states of $^{206}$Pb, $^{208}$Pb and $^{210}$Pb (Be 77c). These predicted levels are depicted as dotted lines. The corresponding cross sections and Q-values associated with each state are also quoted. The experimental energies (solid lines) and (t,p) and (p,t) cross sections are given in (Ig 71), (Fl 74) and (La 73).

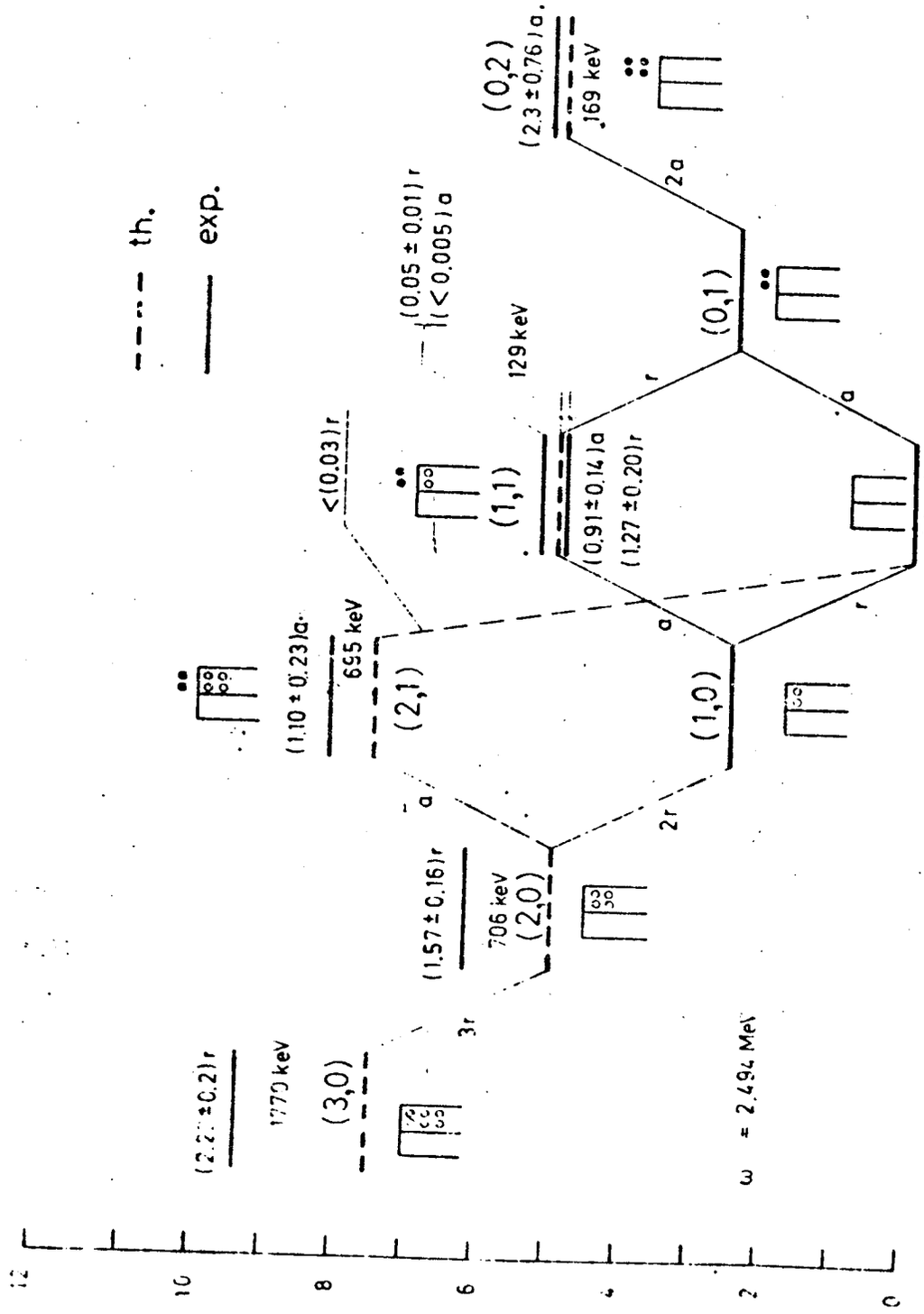
--- th.
— exp.
(0,2)
(2.3 ± 0.76) a
169 keV
2a
(0,1)
(0.05 ± 0.01) r
(< 0.005) a
129 keV
(1,1)
<(0.03) r
(0.91 ± 0.14) a
(1.27 ± 0.20) r
(0,0)
(2,1)
655 keV
(1.10 ± 0.23) a
(1,0)
(1.57 ± 0.16) r
706 keV
(2,0)
(3,0)
1779 keV
(2.2 ± 0.2) r
ω = 2.494 MeV
202
204
206
208
210
212

Fig. III-1

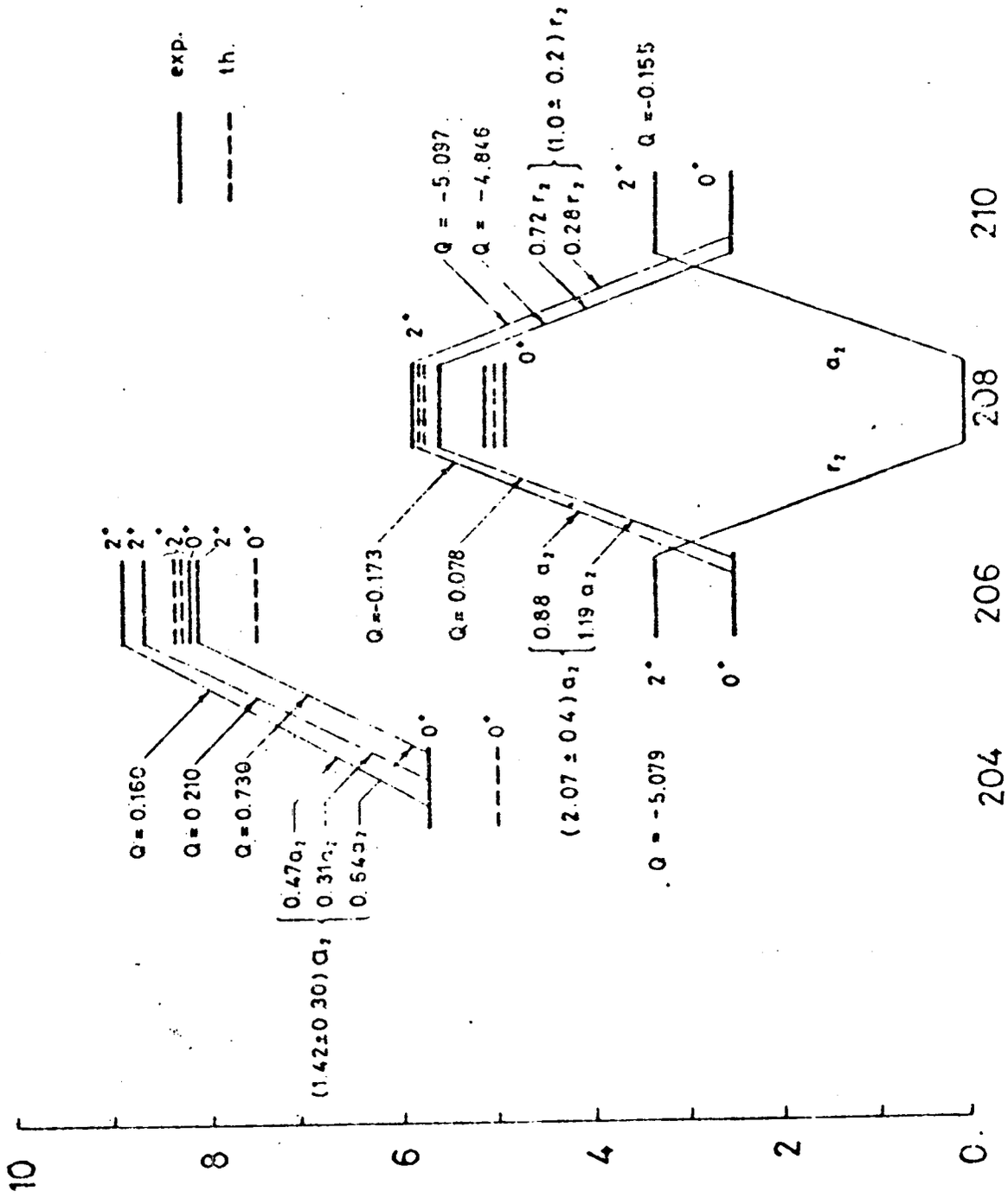
exp.
th.
Q = -5.097
Q = -4.846
0.72 r₂
0.28 r₂
(1.0 ± 0.2) r₂
Q = -0.155
Q = 0.160
Q = 0.210
Q = 0.730
0.47 a₁
0.31 a₁
0.54 a₁
(1.42 ± 0.30) a₁
Q = -0.173
Q = 0.078
0.88 a₁
1.19 a₁
(2.07 ± 0.4) a₁
Q = -5.079
a₁
r₁
204
206
208
210
10
8
6
4
2
0

Fig. III-2

## IV. FEYNMAN'S DIAGRAMS AND THE GRAPHICAL PERTURBATIVE DERIVATION OF THE RPA

In quatum mechanics, we deal with the amplitudes to get from the initial state at time $t$ to the final state at time $t'$. A great advantage of these amplitudes (Green's functions) is that a useful and elegant graphical perturbation theory is obtained from them. Each diagram is as precise as an equation and, in addition, it represents the detailed evolution of the system. In the following, we attempt a fast "derivation" of this technique. For more details see, for instance, (Br 72), (No 64), (Mi 67).

The above mentioned amplitudes, for the one-particle case[+], are

$$G(j',j;t'-t) = -i\langle 0|T\{a_{j'}(t')\, a_j^+(t)\}|0\rangle \qquad (1)$$

where T orders the operators $a_{j'}(t')$, $a_j^+(t)$ in a time sequence that increases from right to left. The creation operators are, in the Heisenberg representation

$$a_j^+(t) = e^{iHt} a_j^+ e^{-iHt} \qquad (2)$$

and $|0\rangle$ is the exact ground state ($H|0\rangle = E_0|0\rangle$). Introducing a complete set of states $|a\rangle$, $|r\rangle$ of the system with one particle more and less than the ground state, eq.(1) reads:

$$\begin{aligned} G(j',j;t'-t) = &\sum_a \langle 0|a_{j'}|a\rangle \langle a|a_j^+|0\rangle e^{-i(E_a-E_0)(t'-t)}\,\theta(t'-t) \\ &- \sum_r \langle 0|a_j^+|r\rangle \langle r|a_{j'}|0\rangle\, e^{-i(E_r-E_0)(t'-t)}\,\theta(t-t') \end{aligned} \qquad (3)$$

---

+ This property of the Green's function becomes apparent if we express (1) in terms of the time evolution operator $e^{-iHt}$. Thus,

$$G(j',j,t'-t) = -i\langle \phi_{j'}(t')|e^{-iH(t'-t)}|\phi_j(t)\rangle\,\theta(t'-t) - i\langle \Psi_j(t)|e^{-iH(t-t')}|\Psi_{j'}(t')\rangle\,\theta(t-t')$$

where

$$|\phi_j(t)\rangle = a_j^+ e^{-iE_0t}|0\rangle \;;\; |\Psi_j(t)\rangle = a_j\, e^{-iE_0t}\,|0\rangle$$

The corresponding Fourier transform is

$$G(j',j;E) = i \sum_a \frac{\langle 0|a_j|a\rangle \langle a|a_j^+|0\rangle}{(E-E_a+E_o+i\eta)} + i \sum_r \frac{\langle 0|a_j^+|r\rangle \langle r|a_j|0\rangle}{(E-E_r+E_o-i\eta)} \qquad (4)$$

i.e., the poles of the Green's functions yield the energies of the neighboring systems. here $\eta \gtrless 0$.

For a system of independent fermions, $|0\rangle$ represents a Slater determinant. Therefore, the one-body Green's function describes the propagation of a particle above the Fermi level if $t' > t$, and of a hole below the Fermi level if $t' < t$. Assuming a representation which diagonalizes the Hamiltonian

$$G(j',j;t'-t) = G_o(j,t'-t)\,\delta_{jj'}$$

$$G_o(j,t) = (1-n_j)\,\theta(t)\,e^{-i\varepsilon_j t} - n_j\,\theta(-t)\,e^{-i\varepsilon_j t} \qquad (5)$$

$$G_o(j,E) = i(1-n_j)/(E-\varepsilon_j+i\eta) + in_j/(E-\varepsilon_j-i\eta)$$

where $n_j = 0$ if $\varepsilon_j > \varepsilon_F$ and $n_j = 1$ if $\varepsilon_j < \varepsilon_F$.

Using the same formalism, we describe the propagation of a particle-hole pair

$$G_{ph}(jj',j''j''';t'-t) = \langle 0|T\{a_{j'}^+(t')\,a_j(t')\,a_{j''}^+(t)\,a_{j'''}(t)\}|0\rangle =$$

$$= \sum_n \langle 0|a_{j'}^+ a_j|n\rangle \langle n|a_{j''}^+ a_{j'''}|0\rangle\,\theta(t'-t)\,e^{-iW_n(t'-t)} \qquad (6)$$

$$+ \sum_n \langle 0|a_{j''}^+ a_{j'''}|n\rangle \langle n|a_{j'}^+ a_j|0\rangle\,\theta(t-t')\,e^{iW_n(t'-t)}$$

which in the case of a free propagator simplifies to

$$G_{ph}^{(0)}(jj',j''j''';t'-t) = \delta_{jj''}\,\delta_{j'j'''}\,\big[(1-n_j)n_{j'}\,\theta(t'-t)\,e^{-i(\varepsilon_j-\varepsilon_{j'})(t'-t)}$$

$$+ n_j(1-n_{j'})\,\theta(t-t')\,e^{i(\varepsilon_{j'}-\varepsilon_j)(t'-t)}\big] \qquad (7)$$

$$= -\delta_{jj''}\delta_{j'j'''}\,G_o(j,t'-t)\,G_o(j',t-t')$$

A non-interacting particle-hole state behaves like a free phonon, since one may distinguish between them only through their correlations with other particles or holes (i.e., in cases in which they are not free). Therefore, for

future use, we may infer the expression for the propagator of a free boson from (7):

$$G_B(n,t'-t) = e^{-i\omega_n(t'-t)}\theta(t'-t) + e^{i\omega_n(t'-t)}\theta(t-t')$$

$$G_B(n,E) = i/(E-\omega_n+i\eta) - i/(E+\omega_n-i\eta) \qquad (8)$$

If we have a more complicated problem (such as a problem of interacting particles) the propagator may be written as a sum over all the alternative ways in which the particles can go from the initial to the final state. For instance, in the case of a particle-hole pair, the particle and the hole can be scattered from the state $(j''j''')$ to the state $(jj')$ by the interaction[+] $-i\langle jj'''|V|j''j'\rangle$.

The alternative ways are:

i) The particle-hole pair may not be scattered at all (eq.(7)).

ii) The particle-hole pair may be scattered once

$$G^{(1)}_{ph}(jj',j''j''';t'-t) = -i\langle jj'''|V|j''j'\rangle\int d\tau\, G_o(j'',\tau-t)\, G_c(j''',t-\tau) G_o(j,t'-\tau)\, G_o(j',\tau-t') \qquad (9)$$

iii) The particle-hole pair may be scattered twice

$$G^{(2)}_{ph}(jj',j''j''';t'-t) = (-i)^2 \sum_{jajb} \langle jjb|V|jaj'\rangle\langle jaj'''|V|j''jb\rangle \qquad (10)$$

$$\times \int d\tau\, d\tau'\, G_o(j'',\tau-t) G_o(j''',t-\tau) G_o(ja,\tau'-\tau)\, G_o(jb,\tau-\tau')\, G_o(j,t'-\tau)\, G_o(j',\tau-t')$$

Reading from right to left these formulæ mean: the particle-hole pair moves as a free particle and a free hole between t and $\tau$; at $\tau$ the particle-hole pair $(j''j''')$ gets scattered by the interaction into another pair $(jajb)$. Then the pair moves again as a free pair, etc. Thus, there is an immediate graphical interpretation of these expansions (fig.IV-1): a diagram is obtained by connecting vertices (and sources) by means of propagators in accordance with the arrow rotation.

---

+. The factor $(-i)$ appears as a consequence of the expansion of the evolution operator $e^{-iHt}$ in power of the intetaction $V(1,2)$. The matrix elements of $V(1,2)$ are defined

$$\langle jj'''|V|j''j'\rangle = \frac{1}{4}\int d1\, d2\, \psi^+_j(1)\, \psi^+_{j'''}(2) V(1,2)\left[\psi_{j''}(1)\, \psi_{j'}(2) - \psi_{j''}(2)\psi_{j'}(1)\right]$$

Since the Fourier transform of a convolution is the product of Fourier transforms, it is easy to obtain the corresponding expressions for them.

The RPA can also be obtained using the graphical procedure. In the propagation of a particle-hole pair, let us consider only those diagrams in which a particle-hole pair is created and annihilated without interacting with other lines of the diagram. Thus, diagrams (IV-1a), (IV-1b) and (IV-1c) belong to this subset, while (IV-1d) does not. This whole subset of diagrams is taken into account in the Bethe-Salpeter equation

$$G_{ph}(jj',j''j''';t'-t) = G^{(0)}_{ph}(jj',j''j''';t'-t)$$
$$-i\sum_{jajb}\langle ja j'''|V|j''jb\rangle\int d\tau\, G^{(0)}_{ph}(jajb,j''j''';\tau-t)G_{ph}(jj',jajb;t'-\tau) \tag{11}$$

as can be seen by iteration. Using (6) and (7) and Fourier transforming, the following equations must be satisfied by the amplitudes $\langle n|a^+_j a_{j'}|0\rangle$ at the poles corresponding to the energies $W_n$:

$$\langle n|a^+_j a_{j'}|0\rangle = \frac{[(1-n_j)n_{j'} - n_j(1-n_{j'})]}{W_n-\varepsilon_j+\varepsilon_{j'}}\sum_{j''j'''}\langle j'j'''|V|jj'''\rangle\langle n|a^+_{j''}a_{j'''}|0\rangle \tag{12}$$

This can be cast into the familiar matrix equation

$$\begin{pmatrix} A & B \\ B^* & A^* \end{pmatrix}\begin{pmatrix} X \\ Y \end{pmatrix} = W\begin{pmatrix} X \\ -Y \end{pmatrix} \tag{13}$$

where

$$(A) = (\varepsilon_k-\varepsilon_i)\delta((ki),(k'i')) + \langle k'i|V|ki'\rangle \;;\; (B) = \langle i'i|V|kk'\rangle \tag{14}$$

The amplitudes are

$$X(n,ki) = \langle n|a^+_k a_i|0\rangle \;;\; Y(n,ki) = \langle n|a^+_i a_k|0\rangle \tag{15}$$

The linearization results of section II can easily be obtained from (13) if the interaction is separable.

Thus we have learned which diagrams have been taken into account in the replacement of "dressed" particle-hole states by phonons. Indeed, in this

replacement an infinite subset of diagrams have been summed up. But this also implies that many others have been neglected. If more than a particle and a hole line would be present in the initial state, and each pair of particle-hole lines gives rise to a boson, we are neglecting interactions between fermion lines belonging to different pairs. In particular, we are violating the Pauli principle, which is taken into account provided that for a given diagram, those obtained by interchanging the end points of the fermion lines are also considered (see, for instance, fig. VII-5). In section VI we discuss how to improve over these limitations of the RPA, using also a diagrammatic technique.

Fig. IV-1. Diagrams representing the propagation of a particle-hole pair in lowest orders of perturbation theory.

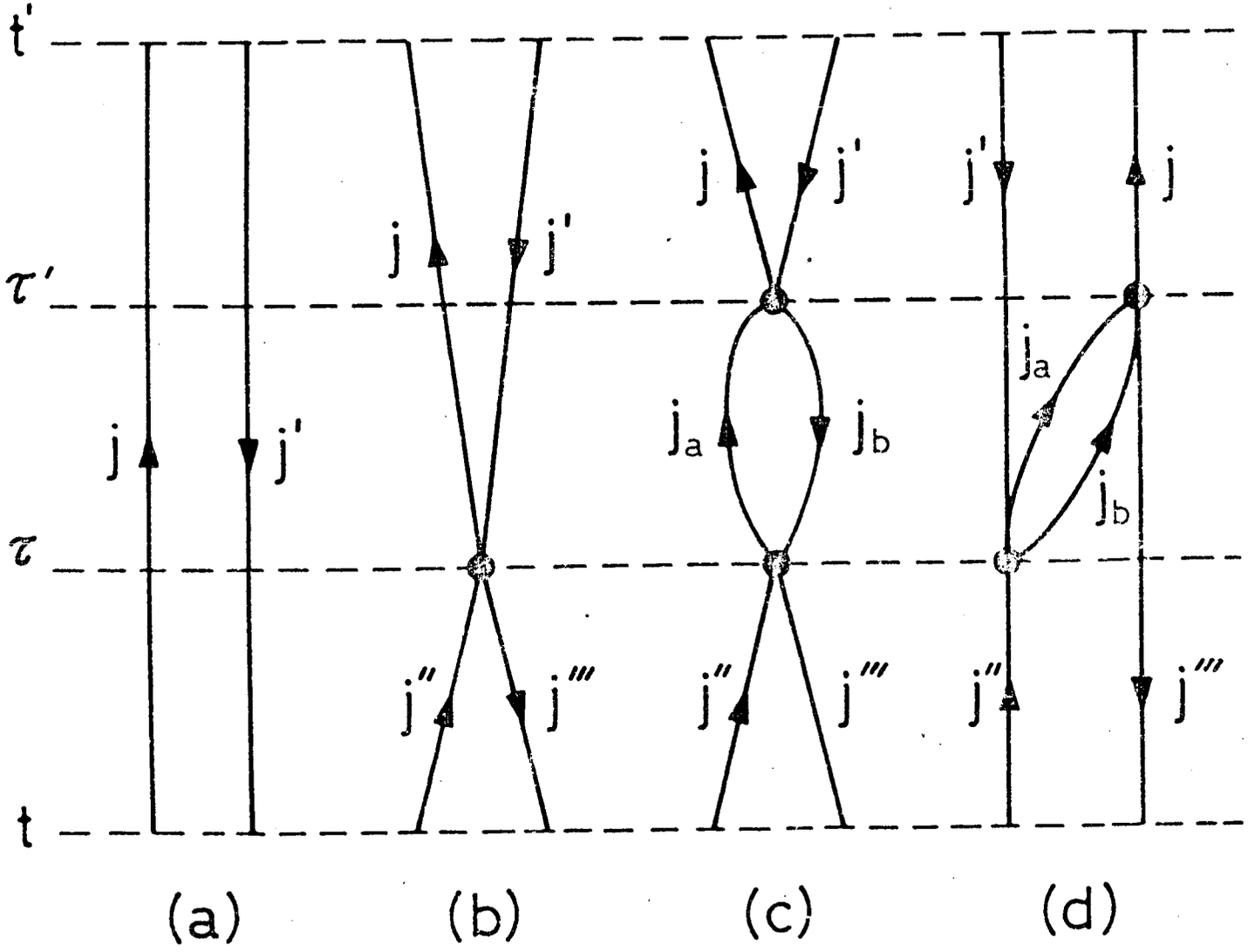
t'
τ'
τ
t
j
j'
j''
j'''
$j_a$
$j_b$
(a)
(b)
(c)
(d)

## V. THE COUPLING BETWEEN ELEMENTARY MODES OF EXCITATION

In the previous lectures we have discussed two elementary modes of excitation of a closed shell system, namely the fermion excitations (which are created by $a_k^+$, $a_i$) and the phonon excitations (which are created by $\Gamma_n^+, \Gamma_{an}^+, \Gamma_{rn}^+$) We must now learn about the interaction between these degrees of freedom. The simplest states in which we may study this interaction have a particle and a phonon, and thus they are excited states of nuclei in the vicinity of close shells (for instance, $Bi^{209}$).

The particle and the phonon degrees of freedom are coupled through the particle-vibration interaction, which has traditionally been assumed to be linear in the boson coordinate and quadratic in the fermion creation and annihilation operators. Thus, one uses the Hamiltonian

$$H = H_o + H_{pv}$$

$$H_o = \sum_{j,m} \epsilon_j a^+_{jm} a_{jm} + \sum_{n\mu} \omega_n \Gamma^+_{n,\lambda\mu} \Gamma_{n,\lambda\mu} \qquad (1)$$

$$H_{pv} = -\sum_n \Lambda_n \sum_\mu (\Gamma^+_{n,\lambda\mu} + (-)^{\lambda+\mu} \Gamma_{n,\lambda-\mu}) Q^+_{\lambda\mu} \qquad (2)$$

where

$$Q_{\lambda\mu} = -(2\lambda+1)^{-1/2} \sum_{j,j'} \langle j \| r^\lambda Y_\lambda \| j' \rangle [a^+_j a_{j'}]^\lambda_\mu \qquad (3)$$

This framework has been extensively used in nuclear physics, ever since suggested in (Bo 52), (Bo 53). However, for a long time only the vertices of figs. (V-1c) and (V-1d) were taken into account. Therefore, the lowest order diagrams contributing to the energy of the particle-phonon state are given in figs. (V-2a), (V-2b) and (V-2c). Their value is

$$\begin{aligned}
\Delta E(2a) &= \left(\frac{2\lambda+1}{2J+1}\right) \Lambda_n^2 \, \delta_{k,J} |\langle k_1 \| i^\lambda r^\lambda Y_\lambda \| k \rangle|^2 / (\epsilon_{k_1} - \epsilon_k + \omega_n) \\
\Delta E(2b) &= (2\lambda+1) \Lambda_n^2 \sum_k \begin{Bmatrix} \lambda & k_1 & k \\ \lambda & k_1 & J \end{Bmatrix} |\langle k \| i^\lambda r^\lambda Y_\lambda \| k \rangle|^2 / (\epsilon_{k_1} - \epsilon_k + \omega_n) \qquad (4) \\
E(2c) &= \sum_{\lambda' k_1} \left(\frac{2\lambda'+1}{2k_1+1}\right) \Lambda_n^2 \, |\langle k_1 \| i^{\lambda'} r^{\lambda'} Y_{\lambda'} \| k \rangle|^2 / (\epsilon_{k_1} - \epsilon_k - \omega_n)
\end{aligned}$$

where J is the total angular momentum of the particle-phonon state.

The appropriate value[+] of the coupling constant $\Lambda_n$ is the one given in (II-15). This can be seen by replacing one of the two factors $Q_{\lambda\mu}$ in (II-12) by its collective version (V-17).

In this period of the particle-vibration calculations, it was also treated the coupling of two particles with the phonon and through a two-body residual interaction (Ra 59); the coupling of phonons and quasi-particles in a superfluid BCS system (Ki 63); etc.

This coupling was employed most frequently in connection with the low-energy quadrupole motion. But it never developed into a great success, because a) in most cases the coupling is so strong that many phonons get admixed in the lowest states, and one gets into difficulties with the estimation of the higher anharmonic effects; b) the coupling term was not properly treated and additional vertices of the fermion-fermion interaction have to be included (as we shall see below); c) insuficient experimental data: only a small fraction of the states belonging to a given multiplet of particle-

---

+ As discussed in section II, the deformed central potential is taken as $V(r) = V_o(r) - R_o \frac{dV_o}{dr}(r) \Sigma \alpha^+_{\lambda\mu} Y_{\lambda\mu}(\theta\phi)$. This yields a coupling term of the form (2), if we assimilate the deformation parameter $\alpha_{\lambda\mu}$ to the quantal coordinate of the collective oscillator. This alternative derivation of the particle-vibration interaction yields results very similar to (2), which is not surprising since: i) the same argument of self-consistency between the deformation of the potencial and the density has been used in the determination of V(r) and in the determination of the coupling strngth $\chi_\lambda$ of the two-body separable interaction; and ii) the detailed radial dependence of the multipole operator is irrelevant to a large extent, provided it is peacked around the nuclear surface. However note that this equivalence can be expected to hold only for linear terms in the phonon coordinates.

phonon states were experimentally known.

The first multiplet to be clearly recognized is the one in $Bi^{209}$ (Ila 66), (Un 71). It is made by a particle in the $h_{9/2}$ state and the octupole phonon of $Pb^{208}$. The empirical level sequence appears in Table V-I, together with the predictions given by eqs. (4). The inadequacy of the coupling becomes apparent+. In this case higher anharmonic effects are not expected to be important, since the splitting of states within the multiplet is small relatively to the phonon energy.

In this older version of the particle-vibration coupling, the shifts in the energy levels are mainly due to the coupling of the particle-phonon state with near lying single-particle configurations. In this case, only the state $i_{13/2}$ has the appropriate spin and parity to be mixed with a state of the septuplet. Consequently, there is only one state, the $J^{\pi}=13/2^{+}$ state, which should be shifted in energy. However, the higher lying states $i_{11/2}$ and $k_{15/2}$ yield a contribution of the same order of magnitude, since the single-particle matrix element of the octupole operator between them and the $h_{9/2}$ state is much larger (no spin-flip is involved).

The coupling scheme works well, however, for other processes. The experimental matrix element for the Coulomb excitation of the single-particle $i_{13/2}$ state (He 69), (Br 70) is reproduced using an effective single-proton charge $(6 \pm 1)e$. This large factor can not be obtained from renormalization effects associated with the giant resonances, which are of order unity. A detailed

---

+ In order to solve this crisis in the history of the particle-vibration coupling, Mottelson (Mo 68) introduced the vertices (V-1a) and (V-1b), in addition to (V-1c) and (V-1d). Superficially, this appears to be incorrect, since their initial and final states are not orthogonal (the boson is a linear combination of particle-hole states and the RPA vacuum includes two-particle two-hole admixtures). In the next chapter, we justify their existence and we show that, in addition, vertices associated with the original two-body interaction have to be also taken into account.

estimate of this renormalized effective charge (Ha 77) yields the value $e_{eff} = 1.2e$.

The particle-vibration coupling contributes in first order to the matrix elements through diagrams (V-3b) and (V-3c). The total contributions of the graphs (V-3) is

$$< k_2 | [Q + Q_{coll}), a^+_{k_1}]^{k_2} |0> = \tag{5}$$

$$= (-)^{k_1-k_2-\lambda} \frac{(2\lambda+1)}{(2k_1+1)^{1/2}} <k_2 \| r^\lambda Y_\lambda \| k_1> e_{eff}\left[1 - \frac{\Lambda_n^2}{\chi_\lambda(\varepsilon_{k_2}-\varepsilon_{k_1}-\omega_n)} - \frac{\Lambda_n^2}{\chi_\lambda(\varepsilon_{k_1}-\varepsilon_{k_2}-\omega_n)}\right]$$

which implies a final effective charge

$$e'_{eff} = e_{eff}\left[1 + \frac{2\Lambda_n^2 \omega_n}{\chi_\lambda[\omega_n^2 - (\varepsilon_{k_2}-\varepsilon_{k_1})^2]}\right] \simeq 6.6e \tag{6}$$

in excellent agreement with the empirical value, (see caption to fig. II-2).

## Appendix

As an example, we proceed to evaluate in detail diagram (2b).

a) The numerator of $\Delta E(2b)$ (eq.(4)) is a product of vertices times racahlogy:

Vertices. In the first interaction, the initial particle is scattered to another particle state and at the same time it emits the final phonon. The vertex has the value:

$$< [\Gamma^+_{n,\lambda} a^+_k]^{k_1} | H_{pv} | a^+_{k_1} > = - \Lambda_n (2\lambda+1)^{1/2} <[\Gamma^+_{n,\lambda} a^+_k]^{k_1} | [\Gamma^+_{n,\lambda} Q_\lambda]^0 a^+_{k_1} >$$

$$= \Lambda_n < k \| r^\lambda Y_\lambda \| k_1> < [\Gamma^+_{n,\lambda} a^+_k]^{k_1} \mid [\Gamma^+_{n,\lambda} [a^+_k a_{k_1}]^\lambda]^0 a^+_{k_1} >$$

$$= \left(\frac{2\lambda+1}{2k_1+1}\right)^{1/2} \Lambda_n < k \| r^\lambda Y_\lambda \| k_1> \quad \text{---} \tag{7}$$

In the second vertex, the initial phonon is absorbed together with the intermediate particle, and a new particle in the $k_1$ state appears. The value of the second vertex is thus the same as for the first vertex.

Racahlogy. The intermediate k particle appears as being coupled to the final phonon in the first vertex, and to the initial phonon in the second vertex. This fact is taken into account by a recoupling coefficient which only depends on the values of the angular momenta. In particular, it is independent if the fermionic or bosonic nature of the entities that are being recoupled. In the present case,

$$< \lambda, (k\,\lambda)k_1\ J | (\lambda k)k_1 \lambda\ ;\ J > = (-)^{J+k}\ (2k_1 + 1) \begin{Bmatrix} \lambda & k_1 & k \\ \lambda & k_1 & J \end{Bmatrix} \qquad (8)$$

After this recoupling, the intermediate particle k appears to be couple to the first phonon in the form $[k\lambda]^{k_1}$. However, if the second vertex is giv by the adjoint of (7), the order of the particle and the phonon must be reversed. This introduces an additional phase $(-)^{\lambda+k-k_1}$. Similarly, the order of the phonon and the particle in the final state of the diagram must be the same as in the initial state. Thus, another phase $(-)^{k_1+\lambda-J}$ in introduced.

Crossings. A factor of minus one has to be included for every crossing between two fermion lines. There are none in the present case.

Summations. A summation over the quantum number of all the intermediate particle and phonon lines has to be performed. In the present case, there is a summation over the intermediate line k. If there are two or more equivalent lines, the result has to be divided by n! where n is the number of equivalent lines[+].

b) Denominators. In the Raleigh-Schroedinger perturbation theory, the denominator is given by the product of the differences between the energy of the initial (final) state and the energy of the intermediate state, $(\varepsilon_{k_1} - \varepsilon_k - \omega_n)$ in the present case. In the Wigner-Brillouin perturbation method, the energy of the initial (final) state is replaced by the perturbed energy E which is being calculated. In this method, the initial or final states can never be intermediate states.

Thus, the value of the diagram (2b) in Raleigh-Schroedinger perturbation

+ Additional factorial factors appear for very special symmetries, for instance, with respect to the time axis (No 64). They occur, for instance, in the case of vacuum diagrams.

theory is given by eq. (4).

Figure captions

Fig. V-1: The particle-phonon vertices.

Fig. V-2: The diagrams contributing to the energy of the particle-phonon state in the order $\Omega^{-1}$.

Fig. V-3: The diagrams contributing to the matrix element of the multipole operator Q between single-particle states.

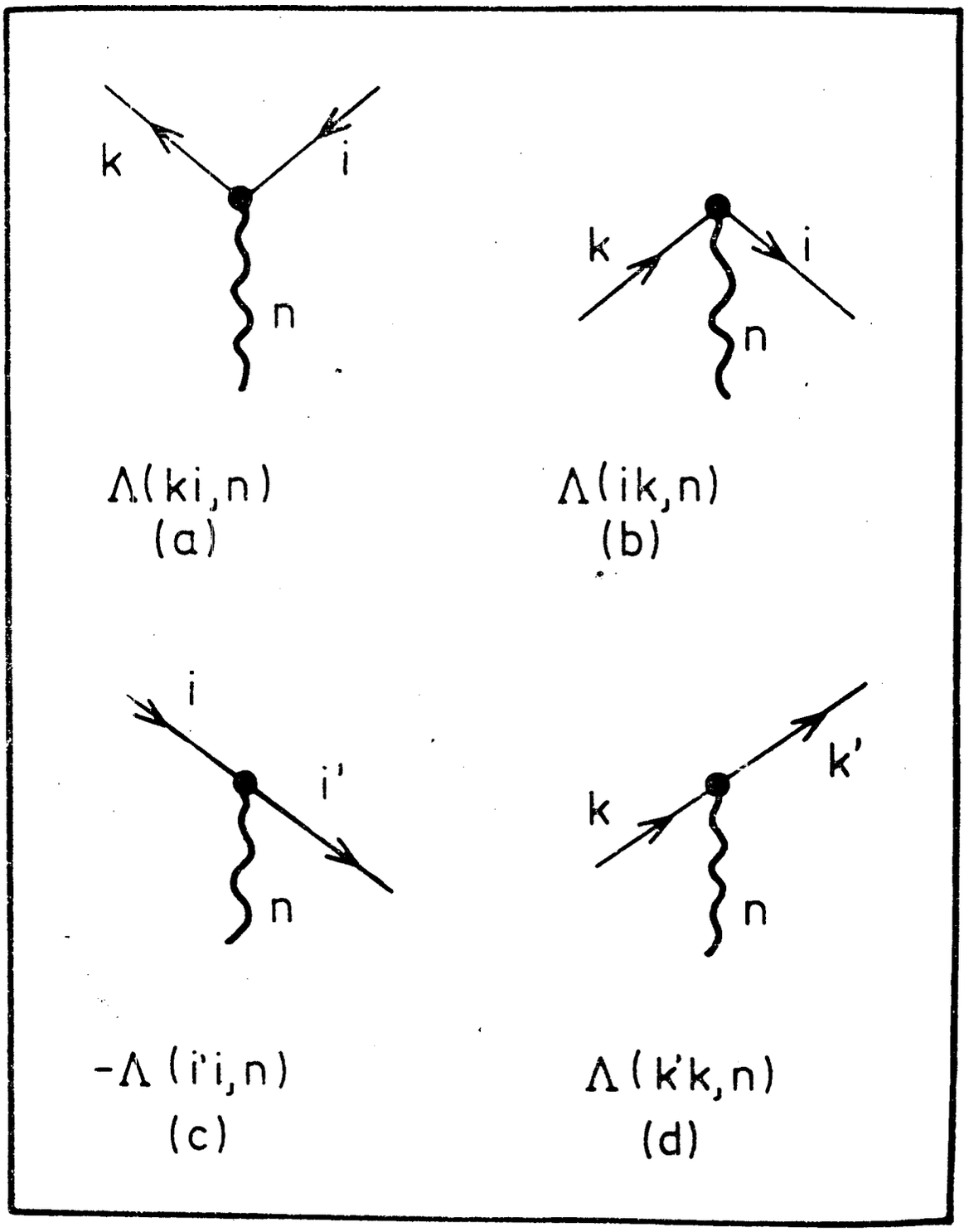
k
i
n
Λ(ki,n)
(a)
k
i
n
Λ(ik,n)
(b)
i
i'
n
-Λ(i'i,n)
(c)
k
k'
n
Λ(k'k,n)
(d)

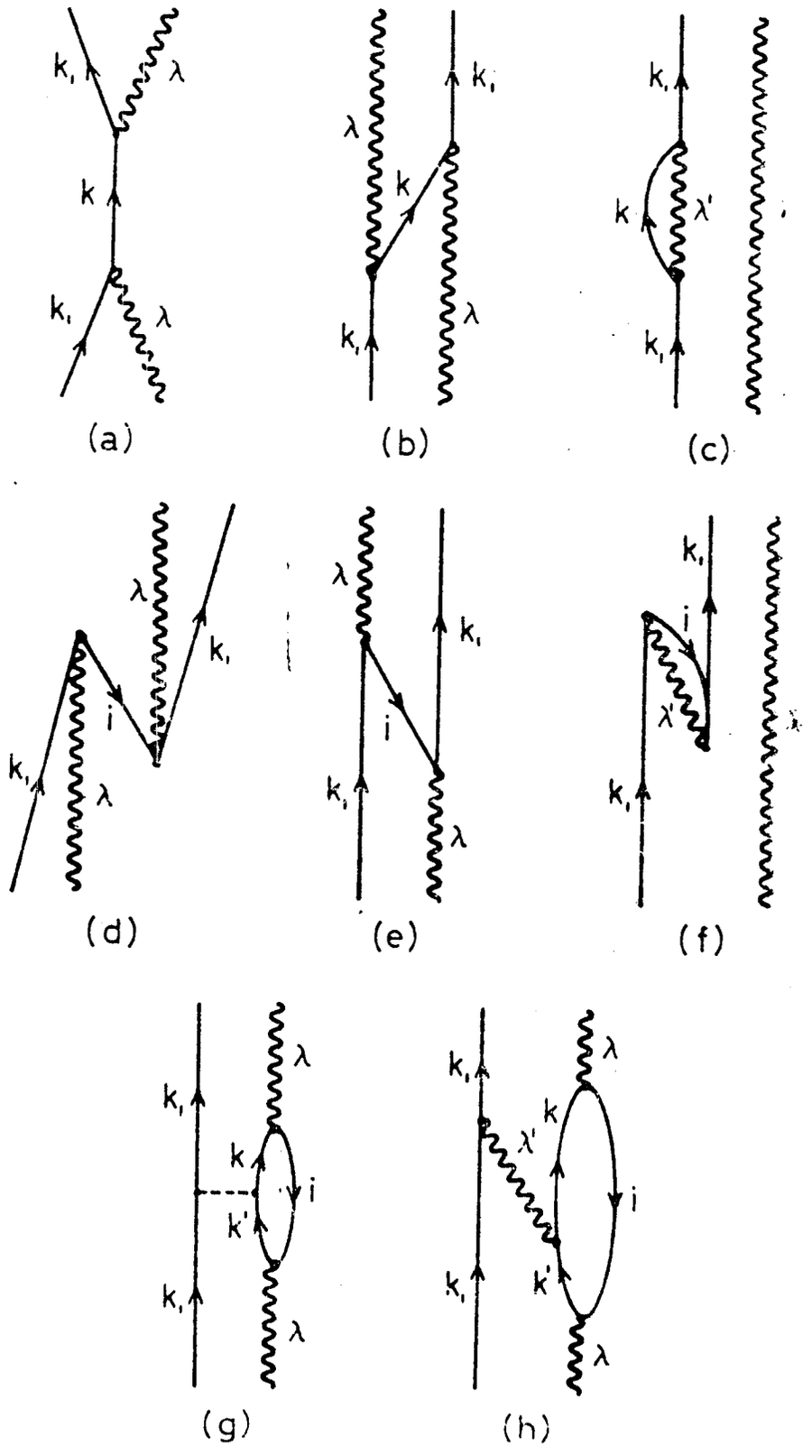
k,
λ
k
k,
λ
(a)
λ
k,
k
k,
λ
(b)
k,
k
λ'
k,
(c)
λ
k,
i
k,
λ
(d)
λ
k,
i
k,
λ
(e)
k,
i
λ'
k,
(f)
k,
λ
k
k'
i
k,
λ
(g)
k,
λ
k
λ'
i
k,
k'
λ
(h)

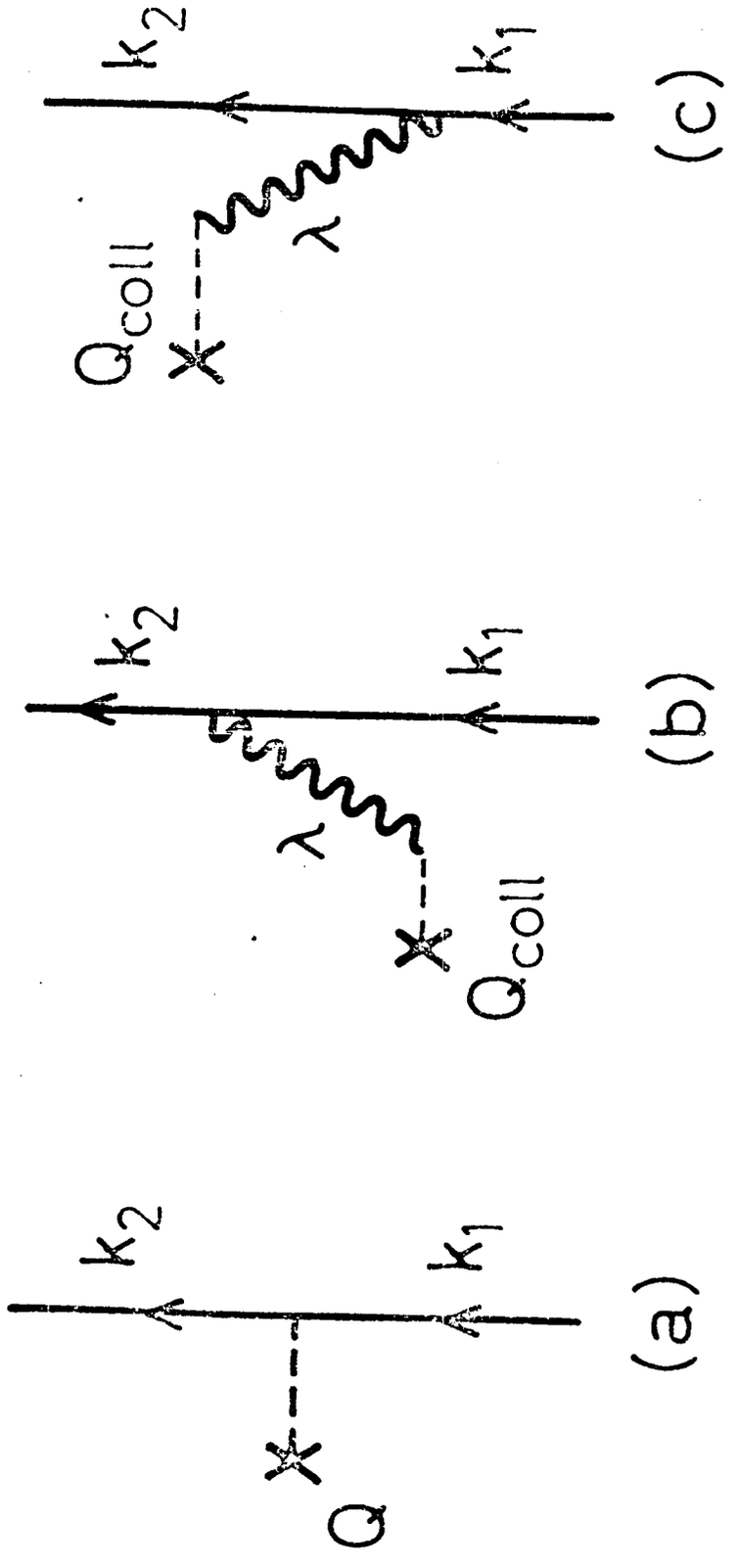


Fig. V-3

| Diagram | $\frac{3}{2}^+$ | $\frac{5}{2}^+$ | $\frac{7}{2}^+$ | $\frac{9}{2}^+$ | $\frac{11}{2}^+$ | $\frac{13}{2}^+$ | $\frac{15}{2}^+$ | Ref. |
|---|---|---|---|---|---|---|---|---|
| (a)+(d) | 129 | 4 | -9 | -5 | -104 | 50 | -49 | Ha 69 |
| (b) | -34 | 11 | -28 | -49 | -32 | -10 | -1 | Ha 69 |
| (e) | 6 | 2 | 46 | -71 | 91 | -128 | 268 | Ha 69 |
| (a)+(b)+(d)+(e) | 36 | 7 | -6 | -89 | -31 | -63 | 156 | Ha 71 |
| (g) | -35 | -18 | -2 | 13 | 21 | 13 | 18 | |
| exp. | -120 | 4 | -29 | -49 | -14 | -14 | 130 | Un 71 |

Table V-I Energy shifts of the members of the septuplet $[\Gamma^+_{3^-} a^+_{h_{9/2}}]^J|0\rangle$ in $Bi^{209}$ (in keV).

We consider now the propagation of two fermion lines in a given Feynman diagram, such that the two lines appear and disappear at different vertices+. The propagation of the two lines yields the Green's function

$$G(j_1t_1, j_a^2t_2\ j_3t_3, j_4t_4)=\langle 0|T\{a^+_{j_1}(t_1)a_{j_2}(t_2)a^+_{j_3}(t_3)a_{j_4}(t_4)\}|0\rangle \qquad (1)$$

If $t_1>t_2>t_3>t_4$ (for instance), the zero and first order contributions to the propagator are

$$G^{(0)}= -G_o(j_4;t_4-t_1)\ G_o(j_2;t_2-t_3)\delta_{j_1j_4}\delta_{j_2j_3} \qquad (2)$$

$$G^{(1)} =-i\langle j_2j_4|V|j_1j_3\rangle \int d\tau\ G_o(j_2,t_2-\tau)G_o(j_1,\tau-t_1)G_o(j_3,\tau-t_3)G_o(j_4,t_4-\tau)$$

Among the second order contributions, we consider the one in which there is a particle-hole pair propagating between $\tau$ and $\tau'$ (fig.VI-1). There are also higher-order contributions in which this intermediate particle-hole pair is scattered an arbitrary number of times by the interaction. The propagation between $\tau$ and $\tau'$ is given by the Green's function (IV-6).

$$\sum_{\nu\geq 2} G^{(\nu)}=(-i)^2 \sum_{jj'j''j'''} \langle j_2j|V|j_1j'\rangle\langle j''j_4|V|j'''j_3\rangle\int d\tau\ d\tau'\ G_o(i_2,t_2-\tau')$$

$$G_o(j_1,\tau'-t_1)\ G_o(j_3,\tau-t_3)\ G_o(j_4,t_4-\tau)G_{ph}(j_2j_1,j_3j_4;\tau',\tau) \qquad (3)$$

By replacing (IV-6) and (IV-15) into (3), we obtain

$$\sum_{\nu\geq 2} G^{(\nu)}=(-i)^2\int d\tau\, d\tau'\ G_o(j_2,t_2-\tau')G_o(j_1,\tau'-t_1)G_o(j_3,\tau-t_3)G_o(j_4,t_4-\tau) \qquad (4)$$

$$\times \sum_n\{\Lambda(j_2j_1;n)\Lambda(j_3j_4;n)e^{-i\omega_n(\tau'-\tau)}\theta(\tau'-\tau)+\Lambda(j_4j_3,n)\Lambda(j_1j_2,n)e^{i\omega_n(\tau'-\tau)}\theta(\tau-\tau')\}$$

where

$$\Lambda(j_aj_b;n) = \sum_{jj'} \langle j_aj|V|j_bj'\rangle\langle 0|a^+_ja_{j'}\Gamma^+_n|0\rangle \qquad (5)$$

---

+ Unlike the propagation considered in (IV-6), where $t_1=t_2$ and $t_3=t_4$.

In (4) the restriction is made that there should be one particle and one hole present in each pair $(j\,j')$.

The partial summation in (4) corresponds to replace the original fermion Hamiltonian by another Hamiltonian in which extra collective degrees of freedom are included.

The factor within curly brackets in (4) has the same time-reversal properties as the propagator of a free phonon with energy $\omega_n$. The summation over $\underline{n}$ accounts for all the diagrams in which a particle and a hole line mutually interact $\nu$ number of times ($\nu \geq 2$). The propagation of each mode $\underline{n}$ is represented by a wavy line. The question whether a wavy line corresponds to the propagation of a true phonon or of a particle-hole pair is irrelevant, since there is no way to distinguish between them: to investigate this difference, another fermion line has to interact with either the particle or the hole line. However, we have assumed that both the particle-hole pair and the phonon propagate without interacting with any other line of the diagram between their creation and annhilation.

The crossing of a wavy line with another line of the diagram (either a fermion line or another wavy line) corresponds to an even number of crossings between fermion lines. Therefore, it does not introduce any extra minus sign, as the crossing between two fermion lines does. This is a further evidence of the identical behavior of the propagators of a boson and a particle-hole pair.

The factors $\Lambda(j_a j_b;n)$ represent the amplitude for the creation and annihilation of a phonon $\underline{n}$ and a single fermion transition from the state $j_b$ to the state $j_a$ (fig.V-1). They should thus be considered as the strength of the particle-phonon interaction. However, these vertices do not exhaust the effects of the two-body residual interaction. In fact, the four-point vertices still give a contribution through $G^{(1)}$. We thus justify the replacement of the fermion Hamiltonian by the nuclear field Hamiltonian introduced in

in (Be 74), namely:

$$
\begin{aligned}
H_f &= H_{sp} + H_{tb} + H_b + H_{pv} \\
H_{sp} &= \sum_j \epsilon_j a_j^+ a_j \quad ; \quad H_b = \Sigma_n \omega_n \Gamma_n^+ \Gamma_n \\
H_{tb} &= \frac{1}{4} \sum_j \langle j_1 j_2 | V | j_3 j_4 \rangle a_{j_1}^+ a_{j_2}^+ a_{j_4} a_{j_3} \\
H_{pv} &= \sum_{nj} \left[ \Lambda(j_1 j_2; n) \Gamma_n^+ a_{j_2}^+ a_{j_1} + \Lambda(j_1 j_2; n) \Gamma_n a_{j_1}^+ a_{j_2} \right]
\end{aligned}
\tag{6}
$$

The exact results of the fermion Hamiltonian are reproduced by (6) provided the following rules are followed:

1) The couplings are allowed to act in all orders to generate the different diagrams of perturbation theory. All vertices of the fermion two-body interaction and of the particle-vibration interaction have to be included, and all time permutations of these vertices in a given diagram have to be taken into account. In particular, the particle-vibration vertices (V-1a) and (V-1b), (Mo 67), have to be considered.

2) The internal lines of diagrams are restricted by the exclusion of diagrams in which a particle-hole pair is created and subsequently annhilated without having participated in the meantime in interaction with another lines (bubles). This rule is due to the fact that all the diagrams with this feature have been replaced by diagrams in which phonons propagate. Because of this rule, only a diagrammatic treatment appears to be feasible.

3) The energies and coupling constants of the phonon field are determined by the energies $\omega_n$ and amplitudes $X(n,jj')$, $Y(n,jj')$ of the perturbed propagator of a particle-hole pair. The simplest method to obtain these quantities is through the RPA (section II). However, we may also use more complicated irreducible vertex parts and, consequently, generalize the concept of buble.

4) It is convenient that the two-body interaction $H_{tb}$ does not contain

Hartree-Fock contributions. These are to be incorporated into $H_{sp}$.

The collective and fermion degrees of freedom are inutually independent.

$$[\Gamma_n, a_j^+] = [\Gamma_n^+, a_j^+] = 0 \qquad (7)$$

$|0>$ is the vacuum the state both for fermions and bosons,

$$\Gamma_n|0> = a_i^+|0> = a_k|0> \qquad (8)$$

There are four possible particle-phonon interaction vertices, according to whether the fermion states $j_a, j_b$ correspond to particles or holes (fig.V-1)

$$\Lambda(ki,n) = <0|a_i^+ a_k H_{pv} \Gamma_n^+|0> = \sum_{k'i'}[< ki'|V|ik'> X(n,k'i') + <kk'|V|ii'> Y(n,k'i')]$$

$$\Lambda(ik,n) = <0|H_{pv}\Gamma_n^+ a_k^+ a_i|0> = \sum_{k'i'}[< ii'|V|kk'> X(n,k'i') + <ik'|V|ki'> Y(n,k'i')] \qquad (9)$$

$$\Lambda(k_1k_2,n) = <0|a_{k_1} H_{pv} a_{k_2}^+ \Gamma_n^+|0> = \sum_{k'i'}[< k_1i'|V|k_2k'> X(n,k'i') + <k_1k'|V|k_2i'> Y(n,k'i')]$$

$$\Lambda(i_1i_2,n) = -<0|a_{i_2}^+ H_{pv} a_{i_1} \Gamma_n^+|0> = \sum_{k'i'}[< i_1i'|V|i_2k'> X(n,k'i') + <i_1k'|V|i_2i'> Y(n,k'i')]$$

where the amplitudes X and Y are defined as

$$X(n,ki) = <0|a_i^+ a_k \Gamma_n^+|0>; Y(n,ki) = <0|a_k^+ a_i \Gamma_n^+|0> \qquad (10)$$

In the formulation of the NFT given in (Be 74) another rule was given, namely that in initial or final states, proper diagrams involve collective modes and particle modes, but not any particle-hole configuration that can be replaced by a combination of collective modes. This restriction permits an initial state of the type $\Gamma_n^+ a_k^+|0>$ , but excludes $a_k^+ a_l^+ a_i^+|0>$. Although correct, this rule is not strictly necessary. It is possible to verify that the matrix elements between proper and improper states vanish identically.

The interaction of the system with an external field is proportional to the one-body operator.

$$Q = \sum_{jj'} <j|Q|j'> a_j^+ a_{j'} \qquad (11)$$

Any fermion diagram that describes the effect of (11) contains two fermion lines (jj') having a common vertex $<j|Q|j'>$ at an instant $t_0$. These two lines

are included within a section of the total diagram, such that this section joins the remaining part of the diagram through the two "external" fermion lines $(j_1 j_2)$ at the instants $t_1$ and $t_2$ $(t_1 \neq t_2)$ respectively (see fig. VI-2). The contribution of this section to the time evolution of the system is

$$G_Q = \Sigma \, \langle j|Q|j' \rangle \, G(j_1 t_1, j_2 t_2, j t_o, j' t_o) \tag{12}$$

In addition to the case of free propagation within the section, let us consider those cases in which the two lines $(j_1 j_2)$ have a common interaction vertex at the time $\tau$, which is also common to the "internal" particle-hole pair, $(j_3 j_4)$. We also assume that $(jj')$ correponds to a particle-hole pair. Applying the same arguments as before eq. (12) can be written in terms of the usual particle-hole Green function $G_{ph}$ which depends on a single time difference $\tau - t_o$:

$$G_Q = -\langle j_2|Q|j_1 \rangle \, G_o(j_2, t_2 - t_o) \, G_0(j_1, t_o - t_1) \tag{13}$$
$$-(-i)\Sigma \, \langle j|Q|j' \rangle \langle j_2 j_4|V|j_1 j_3 \rangle \int d\tau \, G_o(j_2, t_2 - \tau) \, G_o(j_1, \tau - t_1) G_{ph}(j_3 j_4, jj'; \tau - t_o)$$

In order to obtain the field representation of the operator Q, we use in (13) the eqs. (IV-6), (IV-15):

$$G_Q = -\langle j_2|Q|j_1 \rangle \, G_o(j_2, t_2 - t_o) \, G_o(j_1, t_o - t_1) \tag{14}$$
$$-(-i)\int d\tau \, G_o(j_2, t_2 - \tau) G_o(j_1, \tau - t_1) \Sigma_n \left[ \Lambda(j_2 j_1, n) \langle \Gamma_n^+|Q|0 \rangle e^{-i\omega_n(\tau - t_o)} \theta(\tau - t_o) \right.$$
$$\left. + \Lambda(j_1 j_2, n) \langle 0|Q|\Gamma_n^+ \rangle e^{i\omega_n(\tau - t_o)} \theta(t_o - \tau) \right]$$

where

$$\langle \Gamma_n^+|Q|0 \rangle = \Sigma_{ki} \left[ \langle k|Q|i \rangle \, X(n,ki) + \langle i|Q|k \rangle \, Y(n,ki) \right]$$
$$\langle 0|Q|\Gamma_n^+ \rangle = \Sigma_{ki} \left[ \langle k|Q|i \rangle \, Y(n,ki) + \langle i|Q|k \rangle \, X(n,ki) \right] \tag{15}$$

The first term in (14) represents the amplitude for the transition between the single-particle states $(j_1 j_2)$. The second term accounts for a whole set of diagrams in which an initial particle and an initial hole state successively interact.

The coefficients (15) represent the amplitude with which the phonon is created or annihilated by the operator Q.

Therefore, in the field formalism, the operator $Q_f$ contains both a fermion term Q and boson term $Q_b$,

$$\begin{aligned} Q_f &= Q + Q_b \\ Q &= \sum_{jj'} \langle j|Q|j'\rangle\, a_j^+ a_{j'} \\ Q_b &= \sum_n \langle \Gamma_n^+|Q|0\rangle\, \Gamma_n^+ + \Sigma\, \langle 0|Q|\,\Gamma_n^+\rangle\, \Gamma_n \end{aligned} \tag{16}$$

The same arguments can be carried over for the situation in which the succesive interactions take place between two-particle or two-hole lines (pairing phonons). The set of diagrams in which the two lines interact $\nu$ number of times ($\nu \geq 2$) is replaced by a single diagram in which an addition-type or removal type boson is present. The field Hamiltonian (6) is supplemented with the following terms

$$H'_b = \sum_n \left[\omega_{a,n}\Gamma^+_{a,n} + \omega_{r,n}\,\Gamma^+_{r,n}\Gamma_{r,n}\right] \tag{17}$$

$$\begin{aligned} H'_{pv} = \sum_{\substack{n \\ j_1 \geq j_2}} \{ &\left[\Lambda_a(j_1 j_2, n)\Gamma^+_{a,n} + \Lambda_r(j_1 j_2, n)\Gamma_{r,n}\right] a_{j_2} a_{j_1} \\ &+ \left[\Lambda_a(j_1 j_2, n)\Gamma_{a,n} + \Lambda_r(j_1 j_2, n)\Gamma^+_{r,n}\right] a^+_{j_1} a^+_{j_2} \} \end{aligned} \tag{18}$$

where the particle-vibration vertices are

$$\begin{aligned} \Lambda_a(j_a j_b, n) &= \sum_{j \geq j'} \langle j_a j_b|V|jj'\rangle \langle 0|a_j a_j \Gamma^+_{n,a}|0\rangle \\ \Lambda_r(j_a j_b, n) &= \sum_{j \geq j'} \langle j_a j_b|V|jj'\rangle \langle 0|a^+_j a^+_{j'} \Gamma^+_{n,r}|0\rangle \end{aligned} \tag{19}$$

The content of this lecture is based on (Be 76b).

Figure Captions

Fig. VI-1: Correspondence between the Feinman diagrammatic expansion of the propagator in the pure fermion treatment (left) with the Feynman diagrams associated with the same propagator in the NFT (right)

Fig. VI-2: Correspondence between the Feynman diagrammatic expansion describing the effect of an external single operator Q in the pure fermion treatment (left) with the Feynamn diagrams associated with the same process in the NFT (right).

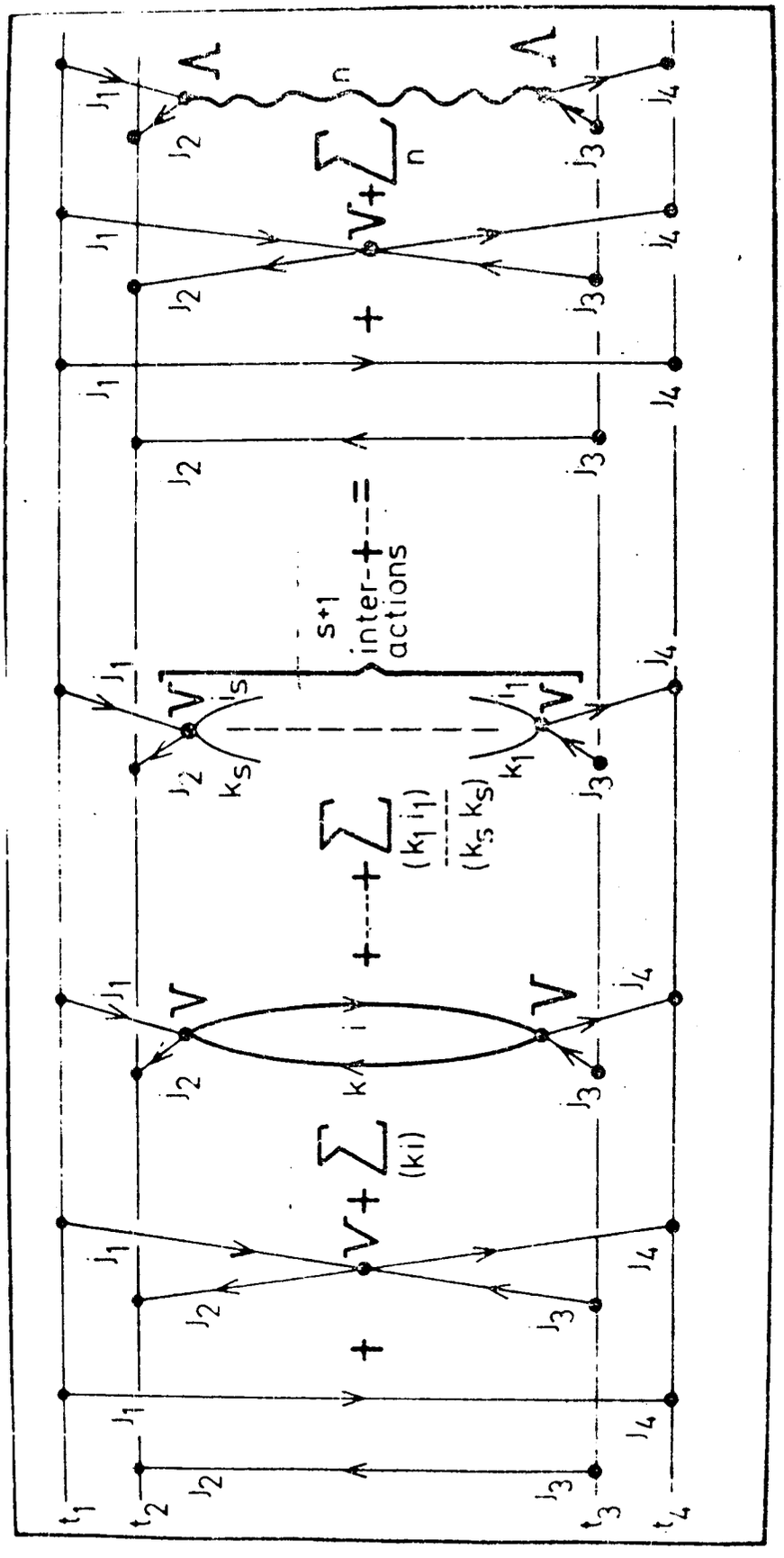


Fig. VI-1

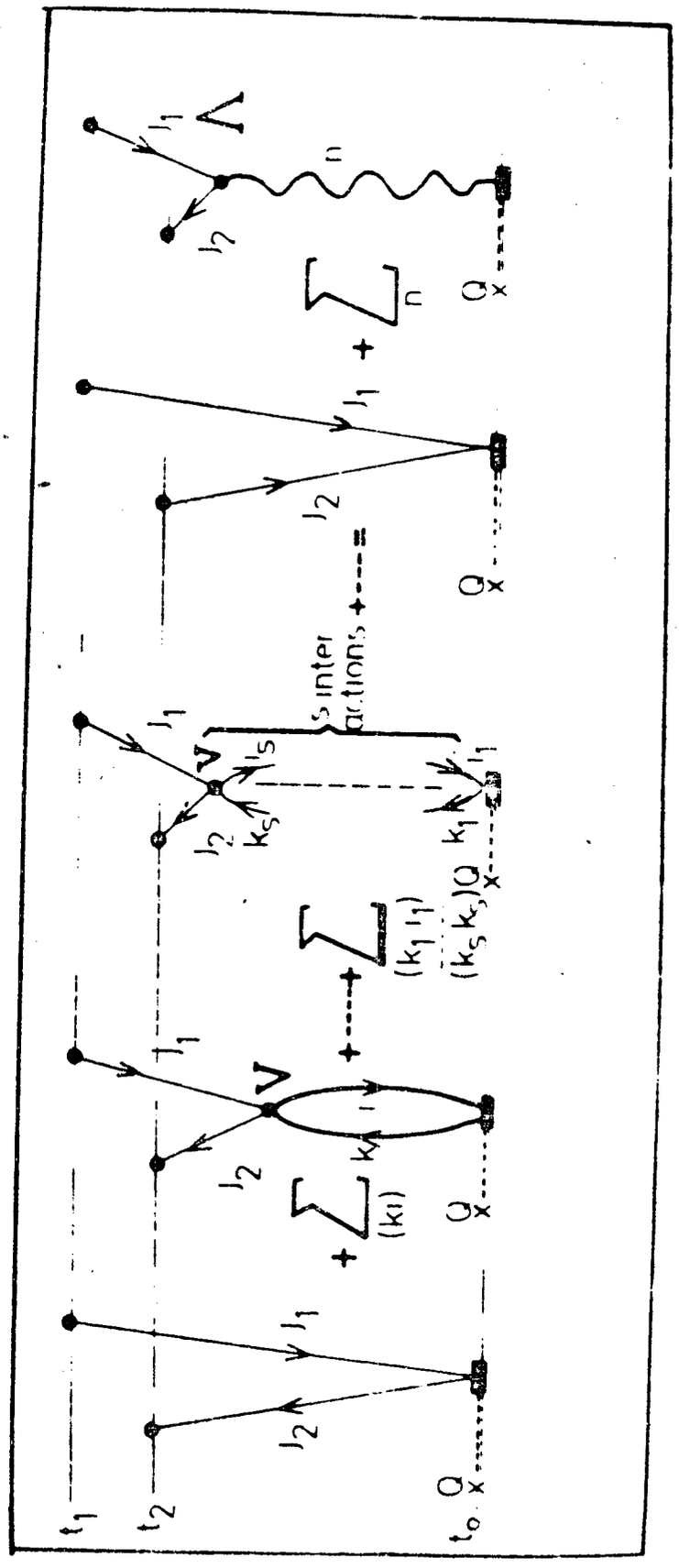


Fig VI-2

## VII. APPLICATION OF THE NFT RULES TO A SIMPLIFIED MODEL CONSISTING OF DEGENERATE PARTICLE-HOLE EXCITATIONS AND A PARTICLE-HOLE MONOPOLE INTERACTION

The fermion Hamiltonian H includes a single-particle term $H_{sp}$ and a two-body interaction $H_{tb}$

$$H = H_{sp} + H_{tb} \tag{1}$$

$$H_{sp} = \frac{1}{2}\,\varepsilon_o (N_1 + N_{\bar{1}}) \tag{2}$$

$$H_{tb} = -\frac{1}{2}\,V\,(A^+A + AA^+) \tag{3}$$

where

$$A^+ = \sum_m a^+_{m1} a_{m\bar{1}} \;;\; N_1 = \sum_m a^+_{m1} a_{m1} \;;\; N_{\bar{1}} = \sum_m a_{m\bar{1}} a^+_{m\bar{1}} \tag{4}$$

The operator $a^+_{m\sigma}$ creates a particle in the state $(m,\sigma)$. The quantum number $\sigma$ ($\sigma = 1$ or $\sigma = -1 = \bar{1}$) denotes either the upper or the lower level. Each level has degeneracy $\Omega$ and the subscript $\underline{m}$ labels each degenerate state. Here, $\varepsilon_o$ is the distance between the two levels and V, the strength of the monopole particle-hole interaction.

The fermion terms in the field treatment include the Hartree-Fock contributions of $H_{tb}$. Since the matrix elements the interaction between the closed shell state and any particle-hole state vanish , the chosen single-particle basis satisfies the Hartree-Fock minimization condition. Consequently, no change in the single-particle wave function is required. However, there is a contribution to the independent-particle energy $\varepsilon_\sigma$, which is defined through the linearization equations

$$\left[H, a^+_{m\sigma}\right]|0\rangle = \varepsilon_\sigma\, a^+_{m\sigma}\,|0\rangle \tag{5}$$

We obtain

$$\varepsilon_1 = -\,\varepsilon_{\bar{1}} = \frac{1}{2}\,(\varepsilon_o + V) \tag{6}$$

and write the pure fermion terms in the field treatment as

$$H'_{sp} = \varepsilon_1 N_1 - \varepsilon_{\bar{1}} N_{\bar{1}} = \frac{1}{2}\,\varepsilon (N_1 + N_{\bar{1}})$$

$$H'_{tb} = -\,V\,A^+A \tag{7}$$

where the Hartree-Fock particle-hole excitation energy is given by

$$\varepsilon = \varepsilon_o + V \tag{8}$$

The only vertex corresponding the interaction $H'_{tb}$ is given in fig. VII-1b. The difference between $H'_{tb}$ and $H_{tb}$ eliminates in this case the Fock single-particle insertions of fig. VII-1a, which are present for the interaction $H_{tb}$.

The pure boson term $H_b$ corresponds to a set of independent phonons

$$H_b = \sum_n \omega_n \Gamma^+_n \Gamma_n \tag{9}$$

with eigenfrequencies $\omega_n$ given by the TDA,

$$\omega_n = \begin{cases} \varepsilon - V\Omega & (n=1) \\ \varepsilon & (n=2,3,\ldots,\Omega) \end{cases} \tag{10}$$

The amplitudes (IV-15) associated with the lowest mode are

$$X(n;m1,m'\bar{1}) = \delta_{m,m'}\Omega^{-\frac{1}{2}} \; ; \; Y(n;m1,m'\bar{1}) = 0 \tag{11}$$

and thus, the particle-vibration interaction reads (eq. (VI-9)):

$$H_{pv} = \Lambda_1 (A^+\Gamma_1 + A\,\Gamma^+_1)$$
$$\Lambda_1 = \sum_{m'} \langle m\,1, m'\bar{1}\,|H_{tb}|\,m'1, m\bar{1}\rangle X(n=1;m'1,m'\bar{1}) = -V\Omega^{-\frac{1}{2}} \tag{12}$$

In the present case, the non-adiabatic phonons ($n \neq 1$) are uncoupled from states involving, for instance, only the adiabatic phonon (n=1) (since the corresponding coupling strengths vanish and the energy denominators do not). In the following, we only treat states involving the adiabatic phonon, and thus we drop the corresponding subindex n = 1.

The sum of terms (7), (9), (12) constitutes the field Hamiltonian $H_f$. One must supplement this Hamiltonian with the diagrammatic restrictions listed in section VI. In the order to perform the diagrammatic perturbation treatment, we divide $H_f$ in two parts

$$H_f = H_o + H' \; ; \; H_o = H'_{sp} + H_b \; ; \; H' = H'_{tb} + H_{pv} \tag{13}$$

The zero-order term includes both systems of independent particles and phonons. The vertices corresponding to H' are given in figs. VII-1b and VII-1c.

The overcompleteness implicit in the product basis is corrected through the perturbative treatment of H'.

If $\varepsilon$ and $V\Omega$ are of the same order of magnitude (which we take to be $0(1)$), a given diagram contributes to a definite order in powers of $\Omega^{-1}$: each vertex (VII-1b) yields a factor $V = 0(\Omega^{-1})$; each vertex (VII-1c), a factor $\Lambda = 0(\Omega^{-\frac{1}{2}})$; and each independent summation over single-particle states, a factor $\Omega$.

The fermion particle-hole transition operator Q must be replaced, within the field treatment, by an operator including both particle and boson terms (eq. (VI-16)). For instance, the operator

$$Q = \sum_m q_m \, a^+_{m1} a_{m\bar{1}} \tag{14}$$

is written as (fig(VII-2)).

$$Q_f = \sum_n \langle n \,|Q|0\rangle \, \Gamma^+_n + Q \tag{15}$$

The definition of a bubble now includes processes in which the particle-hole pair is created by the operator $Q_f$ and destroyed by H', or conversely.

Other operators, such as the one-particle creation or annihilation operators, (which are used in one-particle transfer processes) do not have a boson image.

## The One-Phonon States

Any graph generated by the vertices of figs. VII-1b and VII-1c, and contributing to the energy of the one-phonon state, involves at least a bubble. Therefore, there are no corrections to the TDA energies (10), which coincide with the energies of the fermion treatment.

Similarly, there is a single diagram corresponding to the transition matrix element of the operator $A^+$ between the closed shell and the one-phonon state (fig.(VII-2b)). The TDA value of the vertex and, thus, the value of the transition matrix element is

$$\langle n = 1 \,|A^+|0\rangle = \Omega^{\frac{1}{2}} \tag{16}$$

The one-body transfer operators have no corresponding phonon vertices. Fig. (VII-3) displays the only possible diagram representing the capture of a particle from below the Fermi see, and which is in the same m-state as the initial particle state $|m,1\rangle = a^{+}_{m,1}|0\rangle$. Its contribution is

$$\langle n=1|a_{m\bar{1}}|m,1\rangle = \Lambda/(\omega-\varepsilon) = -\Omega^{-1/2} \qquad (17)$$

The absolute value of this quantitly is also the TDA amplitude of a particle-hole state in the normal mode. Thus, the results of the present subsection do not go beyond (but do not contradict) the values given by the TDA, which already are exact.

The Particle-Phonon States

More interesting from the point of view of the field theory are the particle-phonon states.

In the odd nucleus, the diagram (VII-4b) contributes to the energy of the state with the value

$$-\Lambda^2/(\omega-\varepsilon) = V \qquad (18)$$

which is of the order $\Omega^{-1}$ with respect to the zero-order excitation energy $\omega$. However, unlike the one-phonon case, many other diagrams are possible. For instance, graphs (c) and (d) represent the contributions of order $\Omega^{-2}$. In order to calculate all the higher-order perturbations terms, it is convenient to use the Brillouin-Wigner perturbation expansion. We thus take into account only diagrams in which the initial state is not an intermediate state. Graphs (a), (b), (c), (e),... yield the series expansion W(E), namely

$$W(E) = \omega - \frac{\Lambda^2}{E-\varepsilon} - \frac{\Lambda^2 V}{(E-\varepsilon)^2} - \frac{\Lambda^2 V^2}{(E-\varepsilon)^3} + \cdots$$

$$= \omega - \frac{\Lambda^2}{E-\varepsilon-V} = \omega - \frac{\Omega V^2}{E-\varepsilon-V} \qquad (19)$$

The eq. $E = W(E)$ yields the energies[+]

+ The zero point for the energies in the odd system is placed at $\frac{1}{2}\varepsilon$.

$$E = \begin{cases} \omega + V \\ \varepsilon \end{cases} \qquad (20)$$

Both roots coincide with the exact energies. The second one $\varepsilon$ is also the unperturbed excitation energy of the intermediate two-particle, one-hole state.

In a Feynman diagrammatic expansion of the residual nuclear interaction, intermediate states may violate the Pauli principle. However, for a given diagram in which two fermion lines are simultaneously in the same single-particle state, there is another diagram in which the corresponding end points are interchanged. This second diagram cancels the first one. For instance, in fig. (VII-5a), one of the possible intermediate states has $(m',1) = (m_o,1)$. This intermediate state cannot exist in the presence of an odd-nucleon in the single-particle state $(m_o,1)$. There is another diagram (b) in which the two particle lines of graph (a) are exchanged. The crossing of these two lines introduces a minus sign which cancels the component $m' = m_o$ of the diagram (a) which violates the Pauli principle. The diagrams (a) and (b) are members of two subsets of graphs which are replaced by diagrams (c) and (d), respectively, within the field treatment of the residual interaction. The effect of the process represented in fig. (d) amounts to subtract a component which should not be present in the initial state (c).

Ordinary perturbation theory would predict a negative second-order contribution $\Delta E$ to the energy of the particle-phonon state, since the difference $\omega-\varepsilon$ between the unperturbed energies of the initial and intermediate states is negative,

$$\Delta E = \langle n=1;m_o 1|H_{pv}|m' 1;m'\bar{1};m_o 1\rangle \langle m' 1;m'\bar{1};m_o i|H_{pv}|n=1;\ m_0 1\rangle/(\omega-\varepsilon) \qquad (21)$$

However, diagram (d) (=VII-4b) gives the positive value (18). The second-order contributions which would make $\Delta E<0$ involve bubbles (e). Since these contributions are to be neglected, the correction becomes positive. This does not contradict eq. (21) since the numerator on the right-hand side is positive only for a Hermitian Hamiltonian. Or, although the Hamiltonian (13) appears to be so, it becomes highly non-Hermitian when complemented with the rule concerning the

The square of the amplitude of the initial unperturbed state in the perturbed wave function is given by (Be 77a)

$$(1-\frac{\partial W}{\partial E})^{-1} = \Omega / (\Omega-1) > 1 \qquad (22)$$

The fact that the modulus of an amplitude is larger than one is a further consequence of the non-Hermitian character of the Hamiltonian. The result (22) is consistent with the previous interpretation of diagram (d) since the corresponding contribution eliminates from the phonon a component which should not be there (because of the Pauli principle) : the amplitudes of the remaining components should increase. According to (17),(22) they increase from $\Omega^{-1/2}$ (unperturbed phonon) to $(\Omega-1)^{-1/2}$. One can inmediately see that this last one is the correct amplitude of a single-particle-hole state if the blocking due to the presence of the odd particle is taken into account in the normal mode+.

We proceed to calculate the transition matrix element of the operator $A_f^+$, eqs. (4), (5), from the single-particle state $|m,1>$ to the particle-phonon state $|n=1;m1>$. Since there is no correction to the energy of the single-particle state, the derivative $\frac{\partial W}{\partial E}$ vanishes for the initial state, and the corresponding amplitude equals one. The amplitude of the final state is the square root of (22).

The contribution of all diagrams such that the initial and final states do not appear as intermediate states yields the series expansion (fig. VII-6)

$$< n=1|A^+|0> + \frac{\Lambda}{E-\varepsilon} + \frac{\Lambda V}{(E-\varepsilon)2} + \ldots = \Omega^{1/2} + \frac{\Lambda}{E-\varepsilon-V} = \Omega^{1/2}(1-\Omega^{-1}) \qquad (23)$$

The total matrix element is given by the product of thefinal amplitude times the right-hand side of eq. (23), namely

$$< n=1;m1|A_f^+|m1> = (\Omega-1)^{1/2} \qquad (24)$$

which again expresses the fact that one of the $\Omega$ particle-hole components is blocked in the odd system. The content of the present lecture is taken from (Be 76a)

---

+ The NFT is able to isolate the spurious states that exist in our basis as a consequence of its overcompletness. This is clearly seen in a similar model in which, however, the particle-hole excitations are non-degenerate (Br 76).

Fig. VII-1: Graph (a) represents the Fock self-energy insertions. Graphs (b) and (c) correspond to the four-point vertex of the interaction (3) and to the vertex of the particle-vibration interaction (12) respectively. The value of the vertices is as indicated in the figure, when the particle line appears to the left of the hole line, for all pairs $(m,1;m,1)$ meeting the vertex. A minus sign appears for each interchange of this order.

Fig. VII-2: The two vertices corresponding to a particle-hole operator (eq.(15)).

Fig. VII-3: The diagram representing the population of a phonon state by a single-capture reaction from the system with one more particle than the closed shell.

Fig. VII-4: Energy diagrams for the particle-phonon state.

Fig. VII-5: Graphs (a) and (b) represent sections of two Feynman diagrams which together, take into account the antisymmetry of the intermediate state. Successive interactions between the particle $(m,1)$ and $(m,\bar{1})$ lines give rise to two series of graphs which are obtained in field theory by substituting (c) and (d) in the corresponding sections. Diagram (e) is forbidden.

Fig. VII-6: Diagrams corresponding to the inelastic excitation process in the odd system.

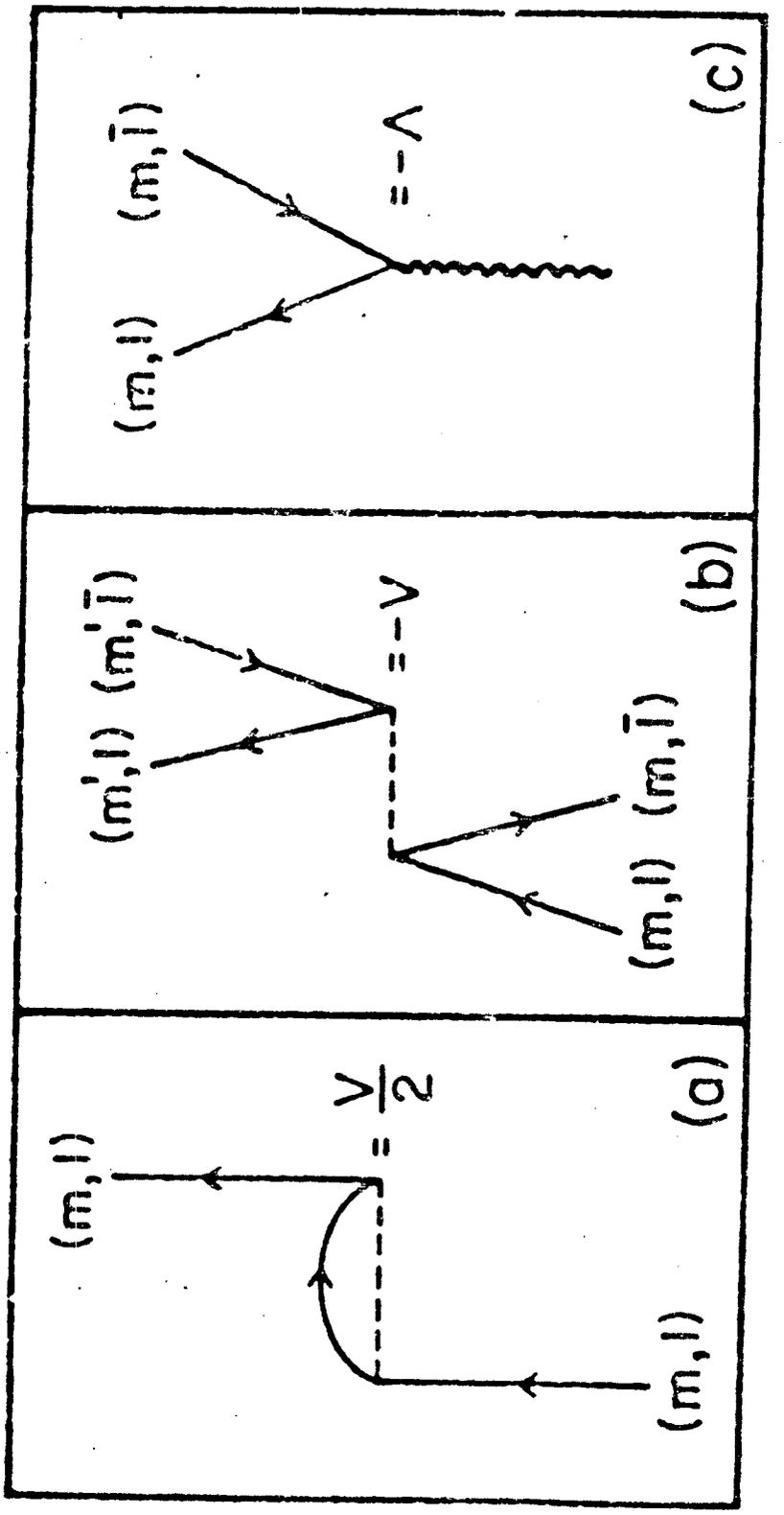


Fig. VII-1

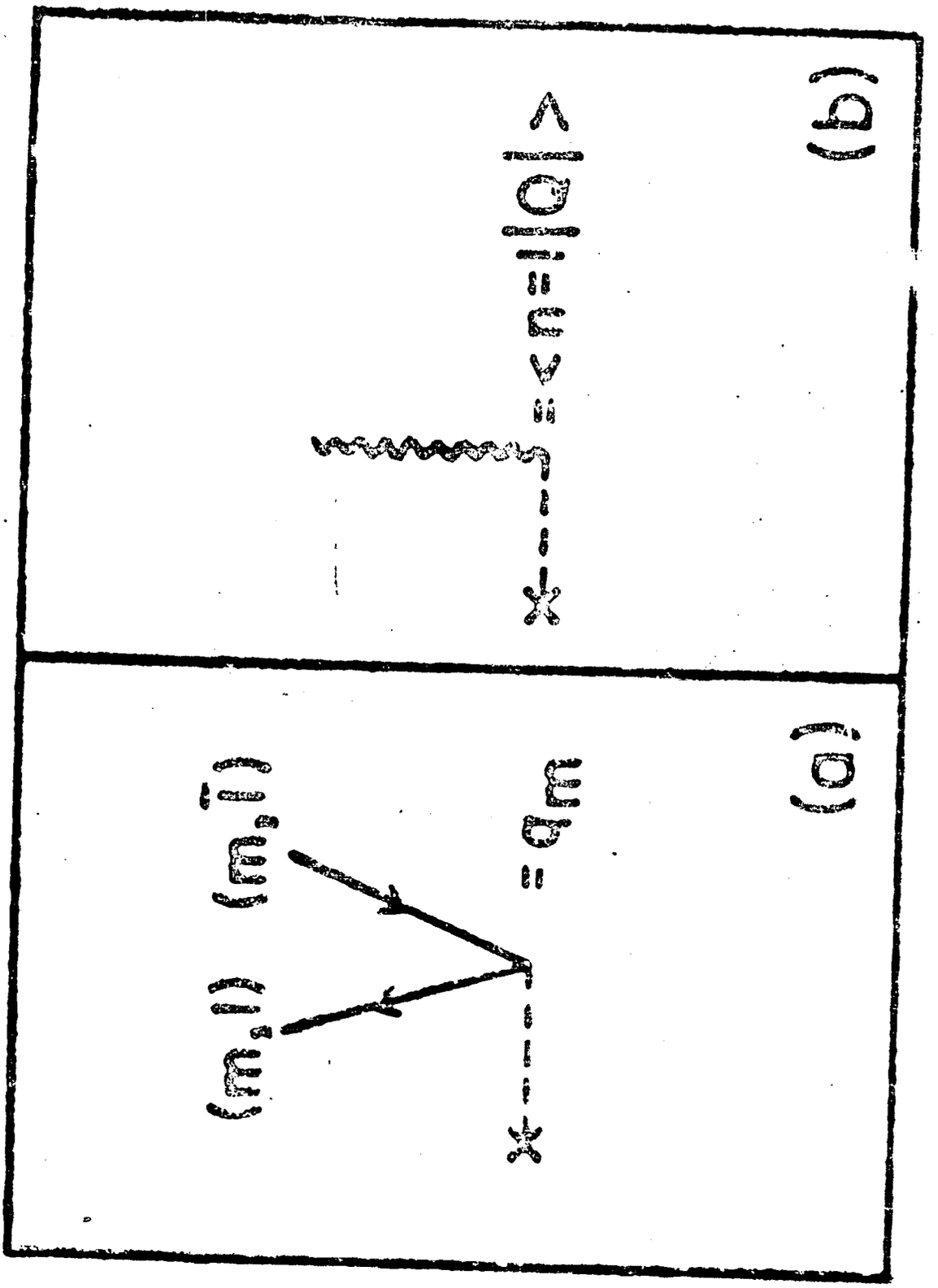


Fig. VII-2

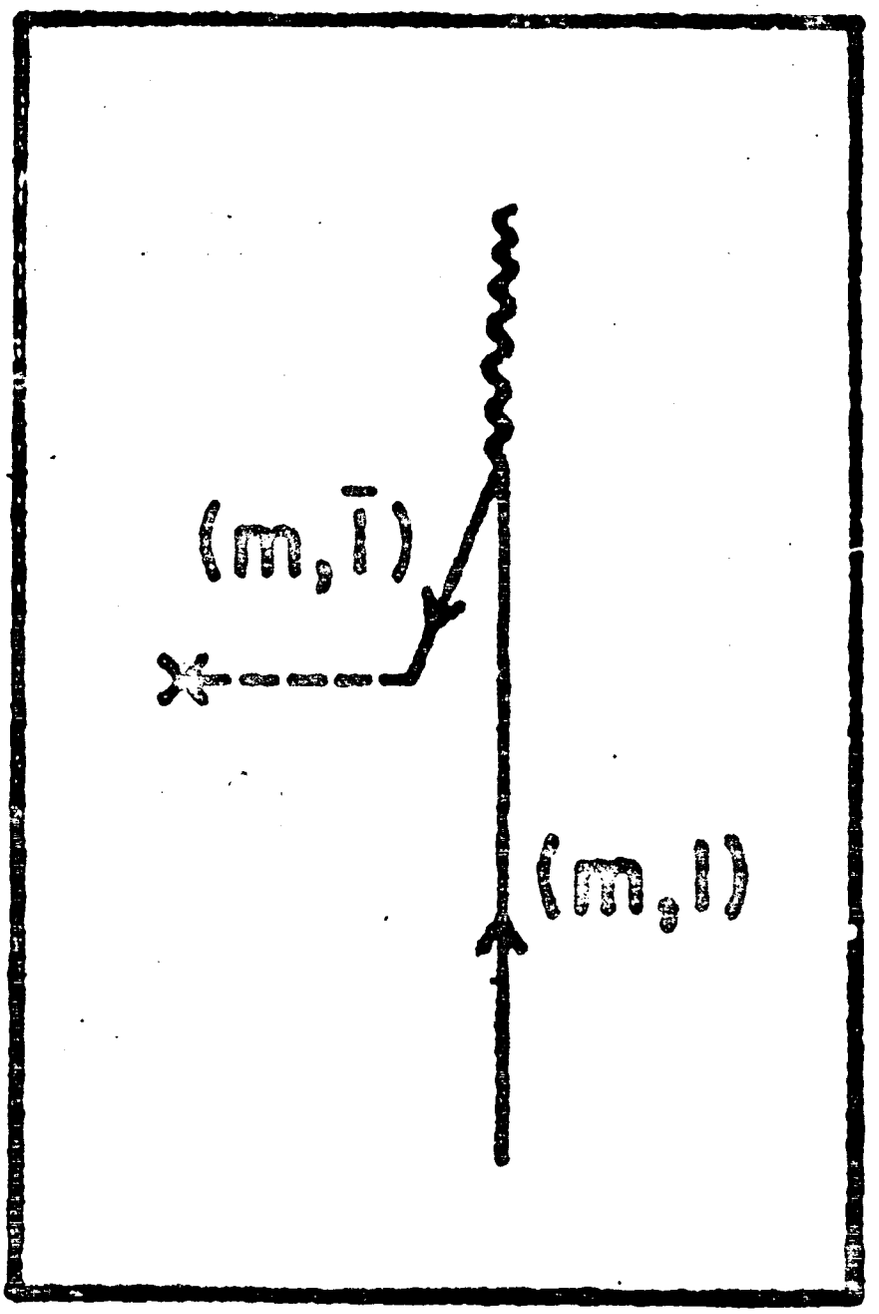


Fig. VII-3

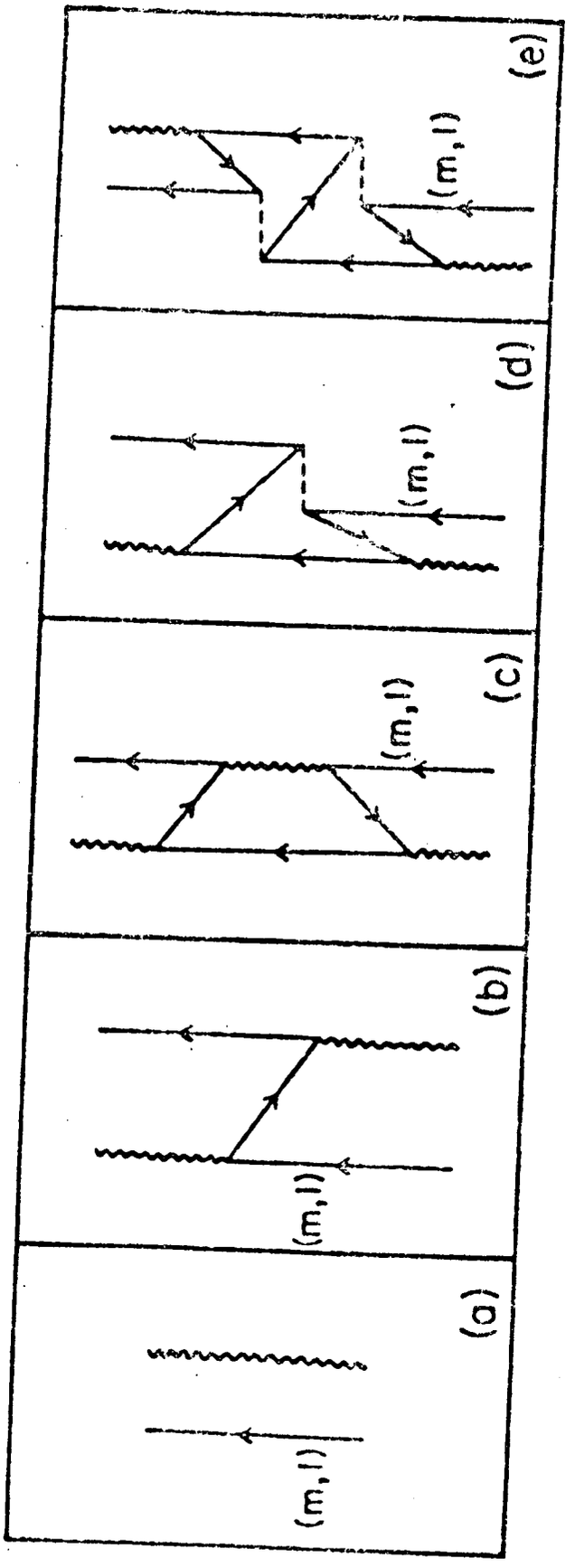


Fig. VII-4

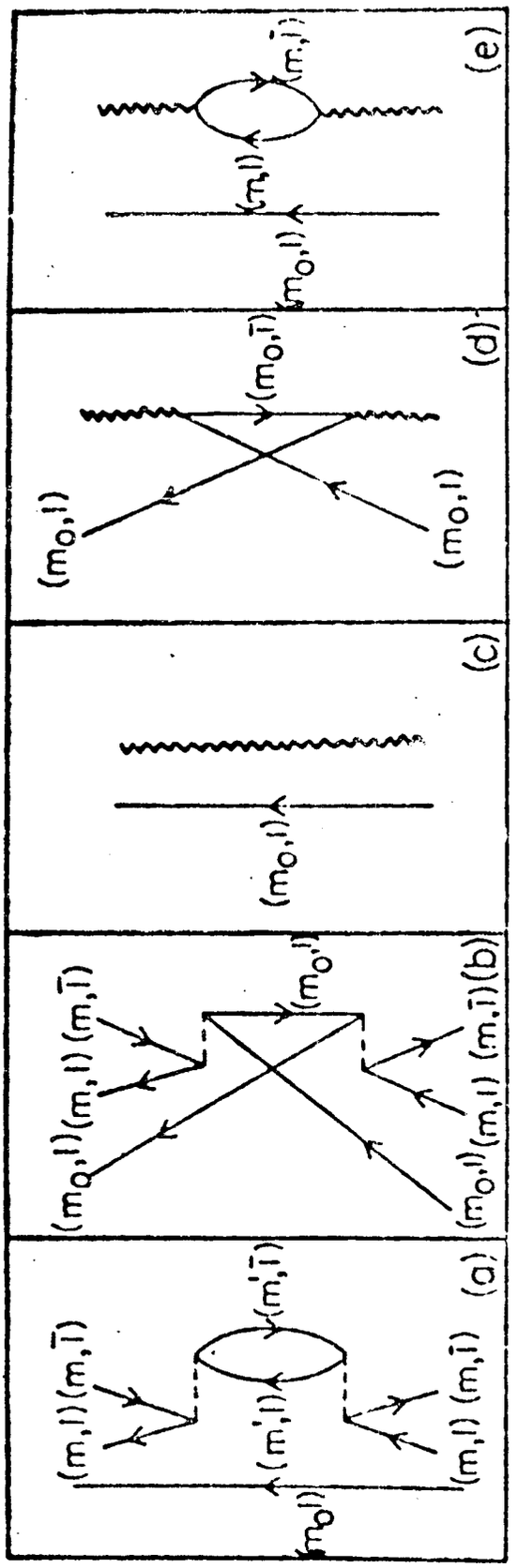
(e)
(m',1̄)
(m,1)
(m₀,1)
(d)
(m₀,1̄)
(m₀,1)
(m₀,1)
(c)
(m₀,1)
(b)
(m₀,1)
(m,1̄)(m',1)
(m₀,1)
(m,1̄)(m',1)
(m₀,1)
(a)
(m',1̄)
(m,1̄)(m,1)
(m',1)
(m,1̄)(m,1)
(m₀,1)

Fig. VII-5

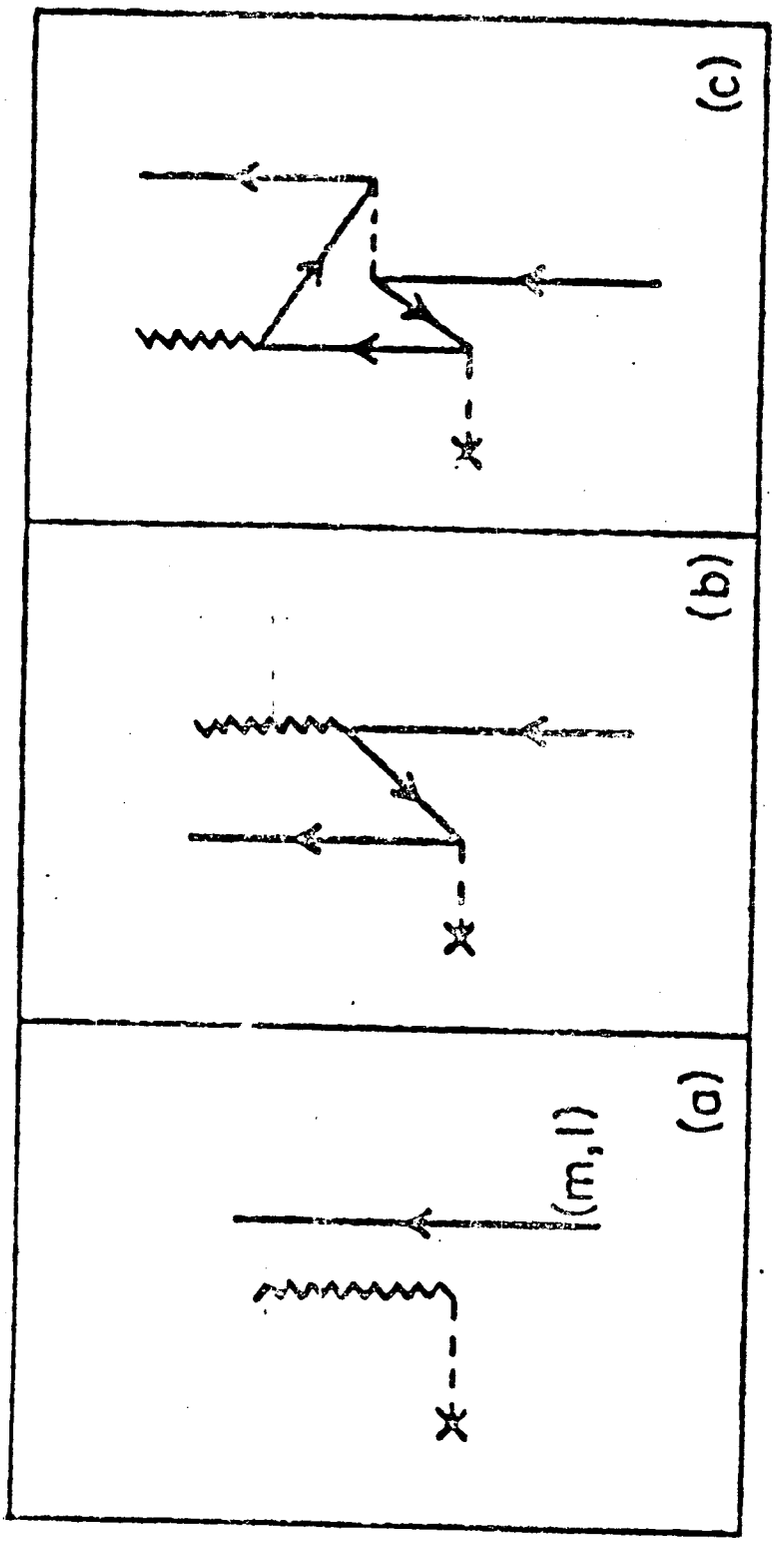


Fig. VII-6

The septuplet of states $[\Gamma_3^+ - e_{h_{9/2}}^+]^J|0\rangle$ in $Bi^{209}$ can not be described in terms of the older version of the particle-vibration coupling model (section V). Because in the new version, the vertices of fig. (V-1a) and (V-1b) are also included, all the time permutations of the vertices in a given diagram have to be taken into account. Thus, one obtains the diagrams (V-2d), (V-2e) and (V-2f) from diagrams (V-2a), (V-2b) and (V-2c), respectively. Their value is

$$\Delta E\ (2d) = -\ (\tfrac{2\lambda+1}{2J+1})\ \Lambda_n^2\ \delta_{i,J} |\langle k_1 \| i^\lambda r^\lambda Y_\lambda \| i\rangle|^2 / (\varepsilon_{k_1} - \varepsilon_i + \omega_n) \qquad (1)$$

$$\Delta E(2e) = (2\lambda+1)\ \Lambda_n^2 \sum_i \begin{Bmatrix} \lambda & k_1 & i \\ \lambda & k_1 & J \end{Bmatrix} |\langle k_1 \| i^\lambda r^\lambda Y_\lambda \| i\rangle|^2 / (\omega_n - \varepsilon_{k_1} + \varepsilon_i) \qquad (2)$$

$$\Delta E(2f) = -\sum_{i,\lambda'} (\tfrac{2\lambda'+1}{2k_1+1})\ \Lambda_n^2\ |\langle k_1 \| i^{\lambda'} r^{\lambda'} Y_{\lambda'} \| i\rangle|^2 / (\omega_n + \varepsilon_{k_1} - \varepsilon_i) \qquad (3)$$

These diagrams were calculated by Hamamoto (Ha 74) who showed that they already yield the correct splitting of the levels in the septuplet (if $J \neq 3/2$).

As discursed in the previous section, the small parameter upon which to expand in the NFT is $\Omega^{-1}$, where $\Omega$ is the number of particle-hole states entering in the construction of the phonon. This number is of the order of the effective degeneracy of the valence shell. In the case of the monopole force, the particle-vibration vertices are proportional to $\Omega^{-1/2}$ and the four-point vertices, to $\Omega^{-1}$. Each independent summation over single-particle states yields a factor of $\Omega$. Although these relative contributions are less clearly defined in the case of a general multipole interaction, we assume that their order of magnitude is the same as for $\lambda = 0$ (i.e., we assume $\lambda \ll \Omega$).

Diagrams (V-2a) and (V-2f) are of order $\Omega^{-1}$ with respect to the unperturbed excitation energy $\omega(3^-)$. We must also include the other diagrams contributing to the same order, to be coherent with our expansion. Thus, the diagrams (V-2g) and (V-2h) (and their time permutations) have also to be taken into account. In order to simplify the calculation, we note that the intermediate boson in fig. (V-2h) must have even parity (i.e., $\lambda = 2,4$) and that, correspondingly, the

effective two-body forces acting in ($\nu i$-2g) are the quadrupole, hexadecapole,... interactions. In the limit in which the energy of the intermediate phonon is large compared to the distance between the levels in the valence shell, the net effect of the intermediate phonon is to renormalize the four-point vertex. Model calculations (Bo 75), (Be 75) indicate that both the quadrupole phonons at 4.08 MeV and at ≈ 10 MeV (giant resonance) contribute to the renormalization of $\chi_2$ with an amount similar to the bare value of $\chi_2$. Therefore, the diagram (V-2h) is taken into account by diagram (V-2g) if one uses the effective value of $\chi_2$ which is necessary to locate the lowest $2^+$ state at the experimental energy 4.08 MeV, using the same set of single-particle levels as in fig. II-2.

$$\Delta E\ (V\text{-}2g) = (2\lambda+1)^{-}\chi_{\lambda'}\Lambda_n^2 \sum_{ii'} \langle k_1 \| i^{\lambda' r^{\lambda'} Y_{\lambda'}} \| k_1\rangle\langle k' \| i^{\lambda' r^{\lambda'} Y_{\lambda'}} \| k\rangle\langle k \| i^{\lambda r^{\lambda} Y_{\lambda}} \| i\rangle\langle i \| i^{\lambda r^{\lambda} Y_{\lambda}} \| k'\rangle$$

$$\begin{Bmatrix} \lambda & \lambda & \lambda' \\ k_1 & k_1 & J \end{Bmatrix} \begin{Bmatrix} \lambda & \lambda & \lambda' \\ k' & k & i \end{Bmatrix} / (\omega_n - \varepsilon_{k'} + \varepsilon_i)(\omega_n - \varepsilon_k + \varepsilon_i) \qquad (4)$$

Nevertheless, it can not be expected that this set of diagrams yields a large contribution, since there is a cancellation between the graphs which involve a particle-particle interaction and those which involve a particle-hole interaction. The resultant values are given in table V-I.

Except for the $J^\pi = 3/2^+$ case, the calculated shifts and level ordering are in agreement with the observed ones (Un 71).

The $3/2^+$ member of the multiplet is populated by inelastic scattering and by one body pick-up reaction on $Po^{212}$. In both reactions there is another $3/2^+$ state which is populated with an intensity of the same order of magnitude (Un 71), (Ba 72). In zero order, the inelastic scattering process is expected to populate only states of the septuplet, while the pick-up reaction feeds the state built out of a $d_{3/2}$ hole on $Pb^{210}$. Therefore, in order to account for the properties of the $3/2^+$ member of the septuplet, it is necessary to couple both the particle-hole and the pairing phonons[+]. The empirical evidence points to

---

+ The present theoretical analysis is taken from (Bo 77a).

the fact that the states

$$|1\rangle = \left[ \Gamma^{+}_{\lambda=3} \; a^{+}_{h_{9/2}} \right]^{3/2} |0\rangle$$

$$|2\rangle = \left[ \Gamma^{+}_{a,\lambda=0} a_{d_{3/2}} \right]^{3/2} |0\rangle \qquad (5)$$

are considerably mixed. As usual, $\Gamma^{+}_{\lambda}$ creates a particle-hole phonon, while $\Gamma^{+}_{a,\lambda}$ creates an addition pairing phonon. The unperturbed excitation energy of the states $|1\rangle$ and $|2\rangle$ is 2.615 MeV and 2.733 MeV, respectively. This last number was fixed from the distance between the $d_{3/2}$ and the $s_{1/2}$ holes and by requiring that the state $\Gamma^{+}_{a,0} a_{s_{1/2}} |0\rangle$ is the state at 2.43 MeV, which is populated in the $Po^{210}$ (t,α) reaction with $\ell = 0$ and a spectroscopic factor very close to 2 (Ba 72).

In the following, we use the Bloch-Horowitz perturbation theory+. All diagram of fig. (VIII-1) contribute to the matrix $M_{ab}(E)$. Because of the energy dependence, there is one matrix M(E) for each final root:

$$M(2.48 \text{ MeV}) = \begin{pmatrix} 72 & 226 \\ & 23 \end{pmatrix}$$

$$M(3.08 \text{ MeV}) = \begin{pmatrix} 79 & 400 \\ & 4 \end{pmatrix} \qquad (6)$$

where the matrix elements are given in keV. Processes of order higher than $\Omega^{-1}$ are neglected in the construction of M.

The two final energies (2.479 MeV and 3.079 MeV) are in close agreement with the experimental numbers (2.494 MeV and 2.95 MeV).

The ratio between the two amplitudes $\zeta_1$, $\zeta_2$ of the states $|1\rangle, |2\rangle$ is given

---

+ The complete set of states is divided into the basic subset ($|1\rangle, |2\rangle$) and the complementary space (all the remaining states). The matrix elements $M_{ab}(E)$ between the members of the basic subset can be constructed diagramatically, using only states belonging to the complementary space as intermediate states (as in Wigner-Brillouin perturbation expansion). The dependence on the resultant energies E appears in the denominators, which are products of the differences between the exact energies and the energy of the intermediate states. The energies are the roots of the determinantal equation $|E - M(E)| = 0$.

as usual by the ratio $(M_{11}(E)-E)/M_{12}(E)$. However, the normalization takes into account the admixture of states belonging to the complementary space and is given (Be 77a)

$$1 = \sum_{a,b} \left[\delta_{a,b} - \frac{\partial}{\partial E} M_{ab}(E)\right] \zeta_a^* \zeta_b \qquad (7)$$

The resulting wave functions are

$$\begin{aligned} |I\rangle &= 0.76\ |1\rangle - 0.53\ |2\rangle \\ |II\rangle &= 0.80\ |1\rangle + 1.02\ |2\rangle \end{aligned} \qquad (8)$$

This states are orthonormal, in spite of their appearence. The fact that one of the amplitudes is even larger than one, has the same explanation as for the amplitude (VII-22): the NFT eliminates spurious components in the basis and thus the amplitude of the surviving ones has to be increased.

The most stricking consequence of including both (non-orthogonal) states $|1\rangle$ and $|2\rangle$and to treat them as orthogonal states which are coupled by the NFT rules, is evidenced in the very different ratio of the (d,d') and (t,α) cross sections associated with the two $3/2^+$ states, namely

$$\begin{aligned} R_a &= B(E3, 2.49\,\text{MeV}) \,/\, B(E3, 2.95\,\text{MeV}) = 3.8 \pm 0.8, \\ R_b &= \sigma((t,\alpha), 2.49\text{MeV})/\sigma((t,\alpha), 2.95\text{MeV}) = 0.8 \pm 0.3 \end{aligned} \qquad (9)$$

Because the component $|1\rangle$ carries basically all the inelastic strength while the (t,α) proceeds through the component of type $|2\rangle$, a treatment which neglects the non-orthogonally of the basis predicts $R_a = R_b^{-1}$.

The calculation can also be (erroneously) done on the assumption that in (8), only $|1\rangle$ is populated by the inelastic scattering and only $|2\rangle$ by the capture process. (i.e., taking into account only the zero order diagrams in the matrix element of the operators corresponding to the different reactions). In this case the results would be given by figs. (VIII-2g) and (VIII-2i), from which the ratios $R_a = 1.92/2.13 = 0.90$ and $R_b = 1.2/4.2 = 0.29$ are derived.

The correct procedure requires to take into account diagrams of the inelastic and transfer operator matrices to the same order as those used in the construction

of the energy matrix elements. This is performed in figs. (VIII-2h) and (VIII-2j) which include the values of the different diagrammatic contributions. The resulting theoretical ratios are $R_a = 216/87 = 2.5$ and $R_b = 1.82/2.27 = 0.80$, in much closer agreement with the experimental numbers.

Figure Captions

Fig. VIII-1: All the $1/\Omega$ contributions to the energy matrix elements of the effective Hamiltonian, in the basis spanned by the vectors $|1>$, $|2>$. An arrowed line represents the fermion fields, while a double arrowed line and a wavy line represent the pairing and surface vibration boson. An open circle or an open square stands for the bare particle-hole and pairing multipole interaction (four-point vertices), respectively (from(Bo 77a)).

Fig. VIII-2: The theoretical spectroscopic factor corresponding to the reaction $Pb^{210}$ $(t,\alpha)$ $Bi^{209}$ is given in figs. (g) and (h) for the zero and $\Omega^{-1}$ processes, respectively. The predicted ratio of inelastic cross sections $d\sigma(h_{9/2} \to J)/d\sigma(Pb^{208}(gs) \to Pb^{208}(3^-))$ is given in (i) and (j), respectively. The upper (lower) value corresponds to the 2.48 MeV (3.07 MeV) $3/2^+$ state (from (Bo 77a)).

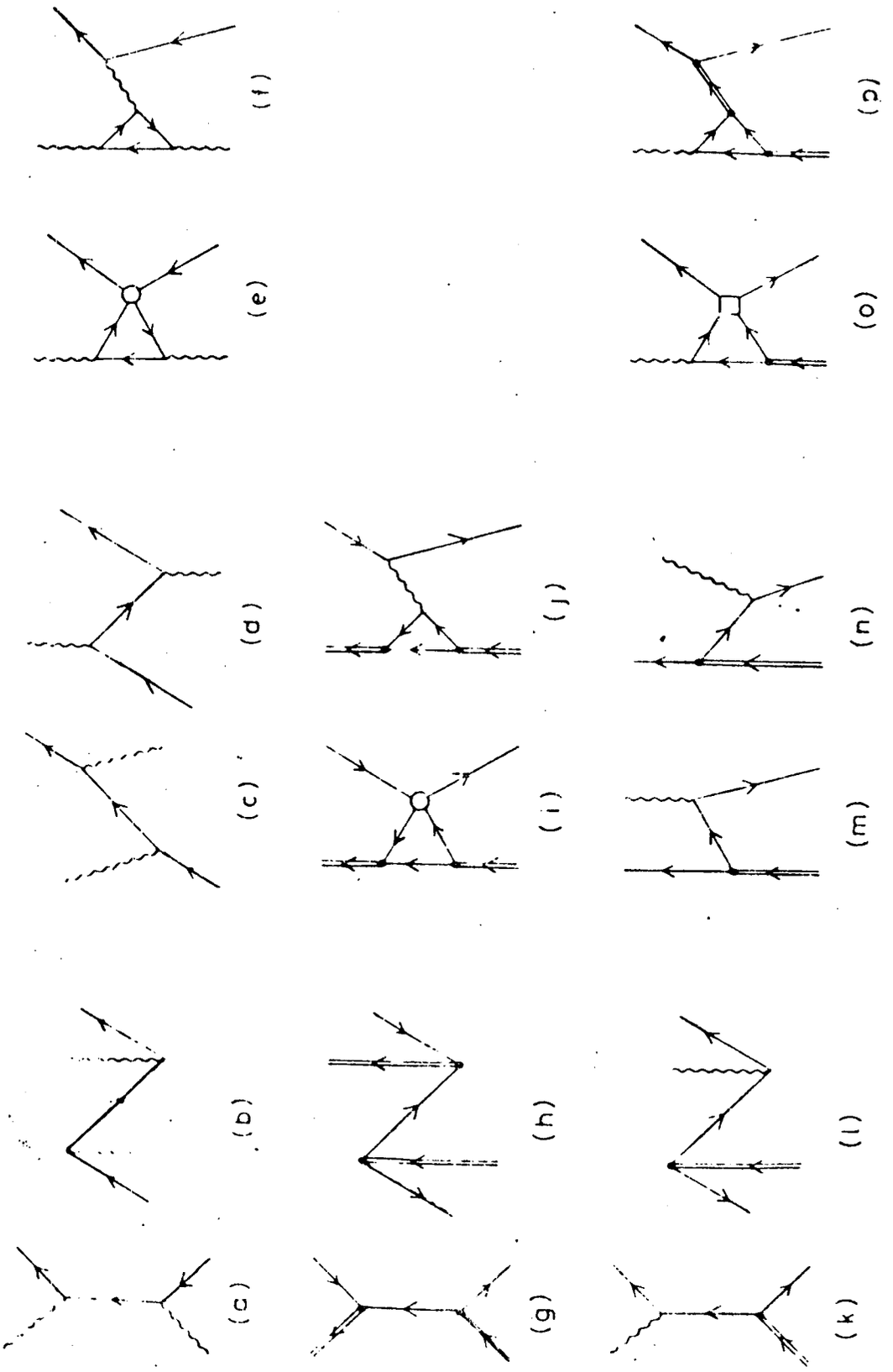


Fig. VIII-1

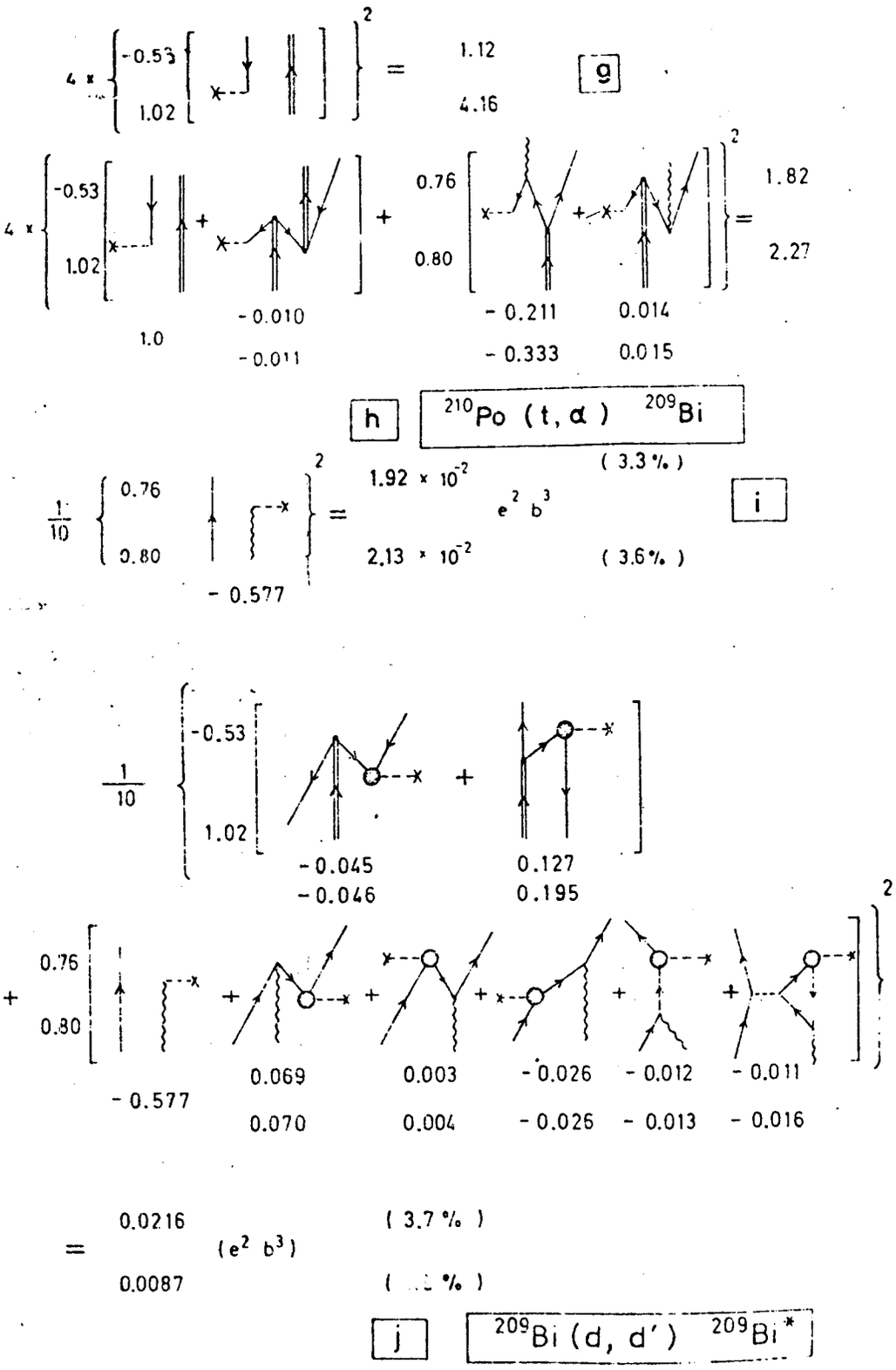
4 × { -0.53 / 1.02 [ ] }² = 1.12 / 4.16
g
4 × { -0.53 / 1.02 [ ] + [ ] } + { 0.76 / 0.80 [ ] }² = 1.82 / 2.27
1.0 / -0.010 / -0.011
-0.211 / 0.014 / -0.333 / 0.015
h
210Po (t, α) 209Bi
1/10 { 0.76 / 0.80 [ ] }² = 1.92 × 10⁻² e² b³ (3.3 %) / 2.13 × 10⁻² (3.6 %)
i
-0.577
1/10 { -0.53 / 1.02 [ ] + [ ] }
-0.045 / -0.046
0.127 / 0.195
+ { 0.76 / 0.80 [ ] }²
-0.577
0.069 / 0.070
0.003 / 0.004
-0.026 / -0.026
-0.012 / -0.013
-0.011 / -0.016
= 0.0216 (e² b³) (3.7 %) / 0.0087 ( .. %)
j
209Bi (d, d') 209Bi*

Fig. VIII-2

## IX. THE TWO-PAIRING PHONON STATES IN $Pb^{210}$ AND $Pb^{206}$

The ground states of $Pb^{210}$ and $Pb^{206}$ can be viewed as the lowest monopole pairing vibrations of $Pb^{208}$. The correlation energy associated with these two modes is 1.237 MeV and 0.640 MeV, respectively. The correlation energy is measured by the difference between the lowest two independent particle (hole) energies $E_\nu$ ($E_\eta$) and the lowest root $\omega_{a,n=1}(\omega_{r,1})$ (c.f. section III). The two-phonon states

$$|I> = [\Gamma^+_{a,1}]^2|0> \qquad (1)$$
$$|II> = [\Gamma^+_{r,1}]^2|0>$$

are the zero order approximation to the ground states of $Pb^{210}$ and $Pb^{204}$, respectively.

An exact diagonalization of the pairing interaction in the Tamm-Dancoff approximation and for a system of four particles (holes) moving around the N = 126 closed shell gives E = 267 keV and E = 540 keV for the interaction energy of states $|I>$ and $|II>$, respectively (the corresponding experimental numbers being 169 keV and 706 keV). Thus, the interaction between the two pairing phonons is of the order of their correlation energy. Consequently, one can expect convergence problems in any perturbative treatment of the interaction.

The NFT results, obtained utilizing the Rayleigh-Schrödinger perturbation expansion, are shown in table IX-I as a function of the expansion parameter $\Omega^{-1}$, $\Omega$ being the effective degeneracy of the valence shells. The strong convergence displayed by the expansion associated with both $\Delta E_I$ and $\Delta E_{II}$ indicates that the NFT partial summations provide with a powerfull technique to deal with strongly anharmonic systems.

However, the interaction with other degrees of freedom (such as surface phonons) requires diagrams of order higher than $\Omega^{-1}$ in the two-pairing-phonon case. In addition, the convergence may be less impressive for smaller degeneracies (such as in the Sr closed shell). The graphical perturbation technique has the disadvantage that the number of diagrams rapidly increases with the

order in $\Omega^{-1}$, both because the number of topologically equivalent diagrams increase as n! where n is the number of vertices, and because the number of topologically inequivalent graphs also increases. For instance, in the particle-phonon case there are 4 of such graphs for $\Omega^{-1}$ and 98 for $\Omega^{-2}$ (Be 76a). In the next section we try to solve this computing difficulty.

| | $\Delta$ E (KeV) | |
|---|---|---|
| Order | I | II |
| $1/\Omega$ | 262 | 474 |
| $1/\Omega^2$ | 4.3 | 42 |
| $1/\Omega^3$ | 0.4 | 14 |
| | 266.7 | 530 |
| Exact | 267 | 540 |

Table IX-1. The two-phonon pairing interaction associated with the (gs($^{212}$Pb) and the (gs($^{204}$Pb)) calculated in the framework of the NFT (Bo 77b).

## X. THE DRESSED PARTICLE AND PHONON LINES

The set of diagrams in which a particle line disappears at a given vertex and subsequently reappears, and such that the intermediate structure does not interact with the remaining part of the graph, may be replaced by a single diagram with a dressed line. The most familiar example of this procedure is the renormalization of a fermion line in the Hartree-Fock approximation. More complicated processes may also contribute, such as the inclusion of a particle-phonon state as intermediate state (figs. (V-2c) and (V-2f). The same is true in the case of phonon lines: the bare particle-hole lines are renormalized in the RPA as discussed in section IV; the phonons may be further dressed by taking into account higher irreducible vertices such as the one shown in fig. (IV-1d).

The renormalization procedure is similar for bosons and fermions. In the following equations, the upper sign refers to bosons and the lower sign to fermions.

The Dyson or Bethe-Salpether equation reads (c.f.eq.(IV-11).

$$G(\ell_2,\ell_1;t'-t) = G_o(\ell_1;t'-t)\,\delta_{\ell_1,\ell_2} - \sum_{\ell\mu} \Lambda(\mu,\ell_1')\Lambda^*(\mu,\ell)\int d\tau\, d\tau'\; G_o(\ell_1,\tau-t)\; F(\mu,\tau'-\tau)\; G(\ell_2,\ell;t'-\tau') \tag{1}$$

where $G_o$ denotes the bare propagator[+]

$$G_o(\ell;t) = e^{-iW_m t}\,\theta(t) \pm e^{-iW_n t}\,\theta(-t) \tag{2}$$

(c.f. (IV-8) and (IV-5)). Here $\ell = m$ for the advanced part and $\ell = n$ for the retarded part.

The matrix elements coupling bare states ($\ell$) with intermediate states ($\mu$) are the vertices $\Lambda(\ell,\mu)$. The propagator F between the times $\tau$ and $\tau'$ depends on the intermediate processes that we intend to consider. For instance the expression for F corresponding to fig. (X-1a) is

---

+ For particle-hole phonons, $W_n = W_m$.

$$F(\mu=(j,n);t) = (1-n_j)\ e^{-i(\epsilon_j+W_n)t}\ \theta(t) - n_j\ e^{-i(\epsilon_j-W_n)t}\ \theta(-t) \qquad (3)$$

These intermediate propagators may be more or less cumbersome to derive, but in principle they may be straightforwardly obtained from the diagrammatic expansion of the intermediate processes. Quite generally, they also have a bosonic or fermionic structure, namely ($\mu=\alpha,\rho$).

$$F(\mu;t) = \phi_\alpha e^{-i\omega_\alpha t}\ \theta(t) \pm \phi_\rho e^{\pm i\omega_\rho t}\ \theta(-t) \qquad (4)$$

The unknowns of our problem are the frequencies and residues of the renormalized propagator

$$G(\ell_2,\ell_1;t) = \sum_a X_a^*(\ell_2)\ X_a(\ell_1) e^{-iE_a t}\ \theta(t) \pm \sum_r X_r^+(\ell_2) X_r(\ell_1) e^{\pm iE_r t}\ \theta(-t) \qquad (5)$$

where

$$X_a(\ell) = \langle a|c_\ell^+|0\rangle \ ;\ X_r(\ell) = \langle r|c_\ell|0\rangle \qquad (6)$$

(c.f.eq.(IV-3) for the fermionic and eq.(IV-6) for the bosonic case).

The dressed line is labelled by an initial $\ell_1$ and a final $\ell_2$ quantum number. It also includes a summation over the numbers indicating the intermediate state (see fig. X-2). The line is created at the vertex $V(\ell_1)$ and annihilated at $V'(\ell_2)$. In the calculation of a given diagram one sums over the three quantum numbers $\ell_1,\ell_2,s$. By performing first the $\ell_1,\ell_2$ summation, one is left with diagrams where the dressed line is labelled only by the quantum number s and is coupled through the vertices

$$\begin{aligned} W(s) &= \sum_\ell V(\ell)\ X_s(\ell) \\ W'(s) &= \sum_\ell V'(\ell)\ X_s^*(\ell) \end{aligned} \qquad (7)$$

Thus, it is convenient to replace the $(\ell_1,\ell_2)$ dressed lines, by those labelled by $\underline{s}$, which have a single pole in the propagator at the energy $E_s$ and are coupled through (7).

In order to determine the energies and amplitudes, we Fourier transform (1) and require analiticity at the poles. The poles at $E_s$ ($s=a,r$) yield a pair

of equations which may be cast in the form a linear eigenvalue problem

$$[A - E + B(E)]X = 0 \tag{8}$$

where

$$A_{\ell\ell'} = W_\ell \sigma_\ell \delta_{\ell\ell'}$$

$$B_{\ell\ell'} = \sigma_\ell \sum_\mu \Lambda^*(\mu,\ell)\ F(\mu,E)\ \Lambda(\mu,\ell')$$

For bosons, $\sigma_\ell = 1$ if $\ell = m$ and $\sigma_\ell = -1$ if $\ell = n$. For fermions, always $\sigma_\ell = 1$. The matrices A, B are of order L, where L is the number of (both positive and negative energy) basic states $\underline{\ell}$ . The determinantal equation associated with (8) is of degree

$$S = L + \mu$$

where $\mu$ is the number of poles in the propagator $F(\mu,E)$. The same kind of non-linear eigenvalue problem arises whenever the full space spanned by the unperturbed states is split into two parts (basic and complementary space) and there is an eigenvalue problem of an energy dependent effective Hamiltonian restricted to the basic space (Bloch-Horowitz perturbation method).

In addition to the energies $E_s$, the matrix equation (8) yields the relative values of the amplitudes $X_s(\ell)$. The normalization of these amplitudes takes into account i) the fact that intermediate states belonging to the complementary space are implicitely mixed with the basic states $\underline{\ell}$ and ii) the characteristic metric of boson states (i.e., the fact that if

$$X_s(\ell) = \begin{pmatrix} X_s(m) \\ X_s(n) \end{pmatrix} \tag{10}$$

is an eigenvector of A + B(E) when this matrix operator acts to the right, the corresponding eigenvector "to the left" is

$$X_s^+(\ell) = (X_s^*(m)\ , \mp X_s^*(n)) \tag{11}$$

A normalization condition satisfying the previous requirement can be obtained by extrapolating the results of (Be 77a) in order to take into account the metric, namely

$$\sigma_s = \sum_{\ell\ell'} \left[ \delta_{\ell\ell'} - \frac{\partial}{\partial E} B_{\ell\ell'}(E) \right] \sigma_\ell \, X_s^*(\ell) \, X_s(\ell')$$

$$= \sum_m |X_s(m)|^2 \mp \sum_n |X_s(n)|^2 \qquad (12)$$

$$- \sum_{\ell\ell'\mu} \Lambda^*(\ell,\mu) \frac{\partial}{\partial E} F(\mu,E) \; \Lambda(\mu,\ell') \; X_s^*(\ell) \; X_s(\ell')$$

This normalization condition is also obtained by requiring the states $|a\rangle$ and $|r\rangle$ to be eigenfunctions of the operator correponding to the number of particles. This is contained in the Ward identity, which states that the electron self-energy and vertex corrections mutually cancel in the limit of low momentum transfer. The limit occurs in a spherical shell model system for a monopole operator with constant matrix elements (i.e., the number of particles operator). For instance, in the fermion case, the matrix element of the number operator is given by the graphs of fig. (X-3). It is easy to verify that the sum of these diagrams yields eq. (12). More details are given in (Be 77b).

Figure Captions

Fig. X-1: Graphical representation of the right hand side in the Dyson (a) and Bethe-Salpether (b), (c) equations. The dressed fermion and pairing phonons are labelled by two arrows, while the dressed particle-hole phonon carries a circle.

Fig. X-2: The propagation of a fermion line, taking into account the succesive emission and absortion of a phonon

Fig. X-3: The vertices of the number operator and the graphical representation of this operator between dressed states.

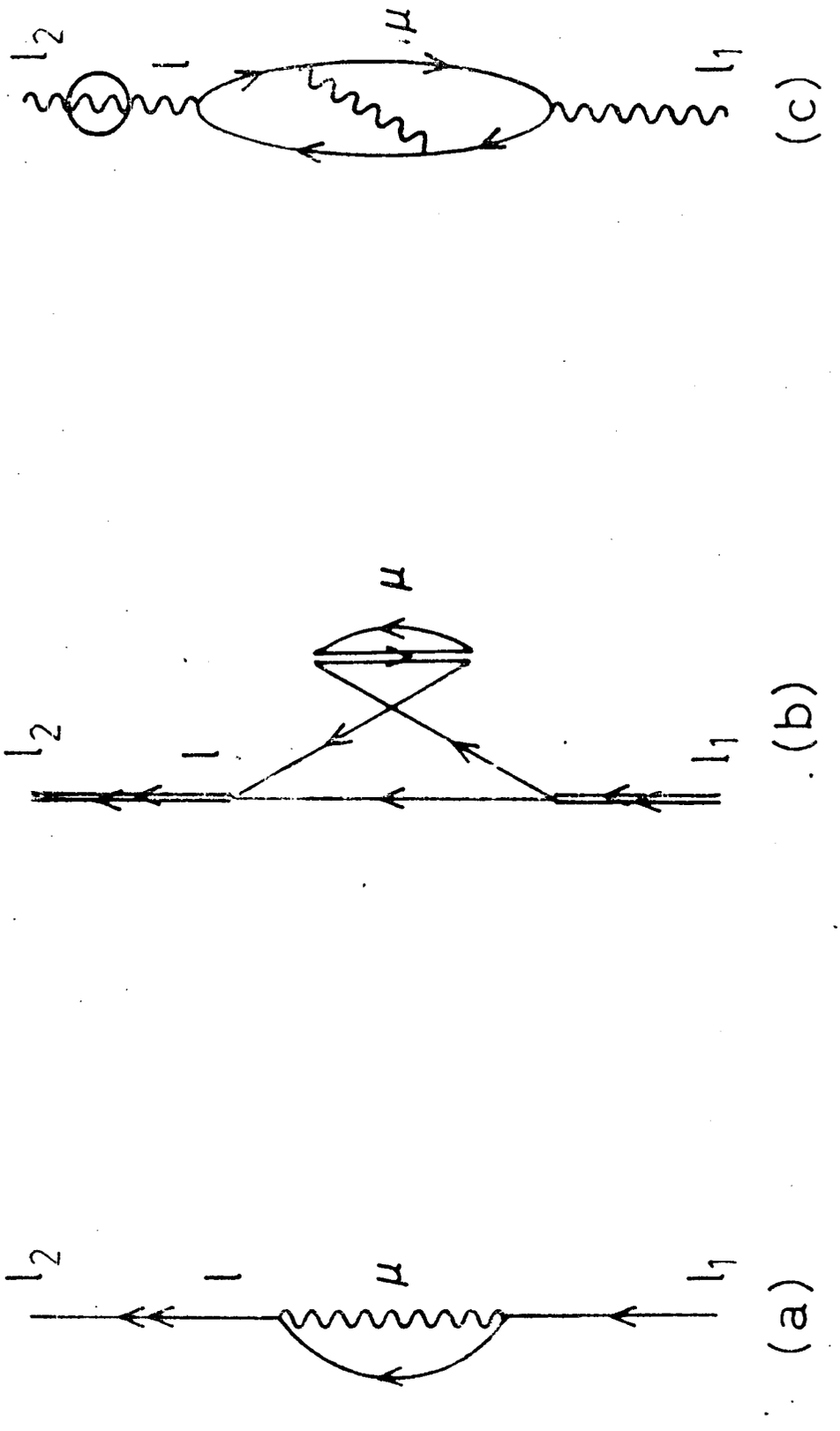


Fig. X-1

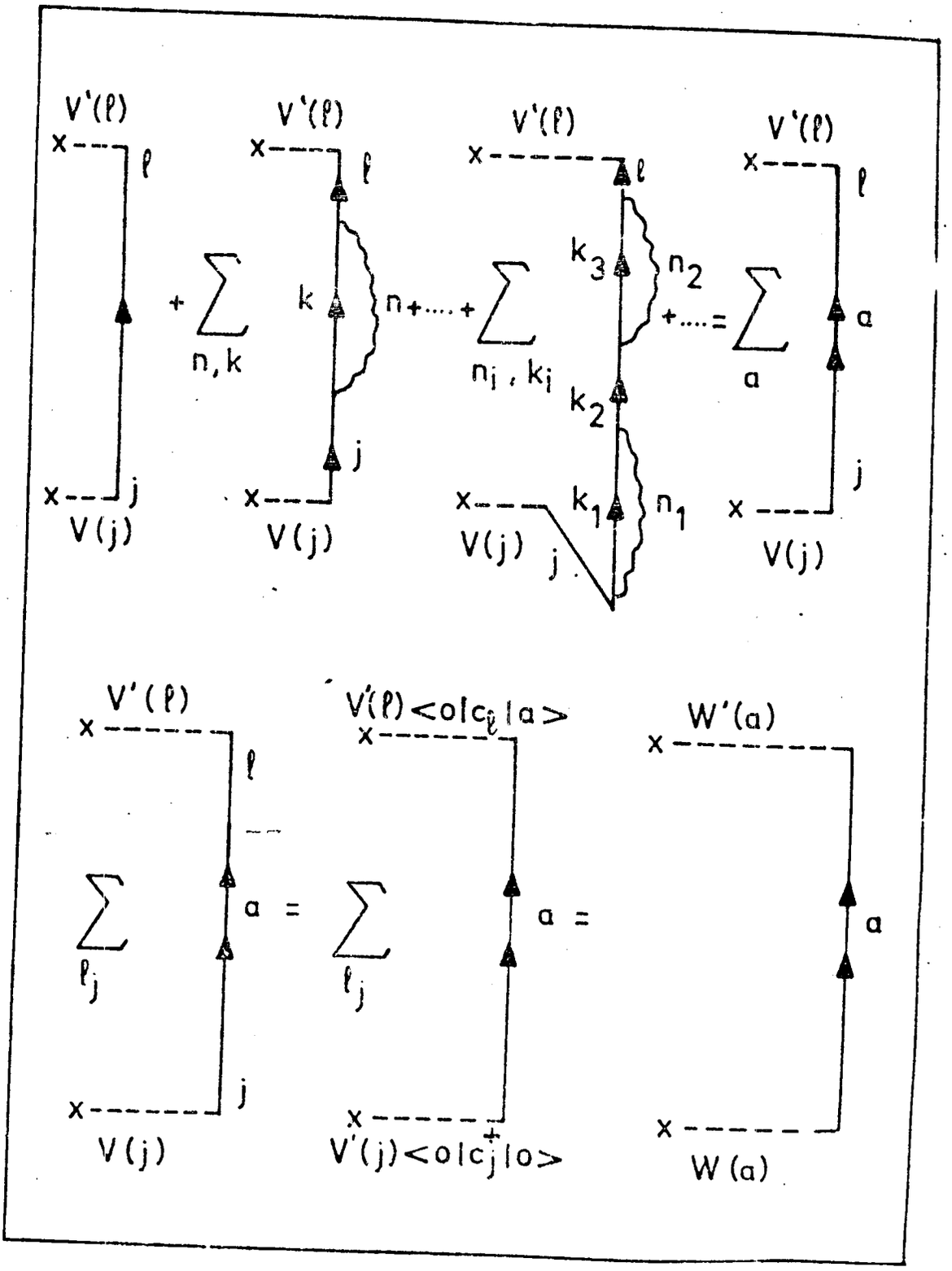


Fig. X-2

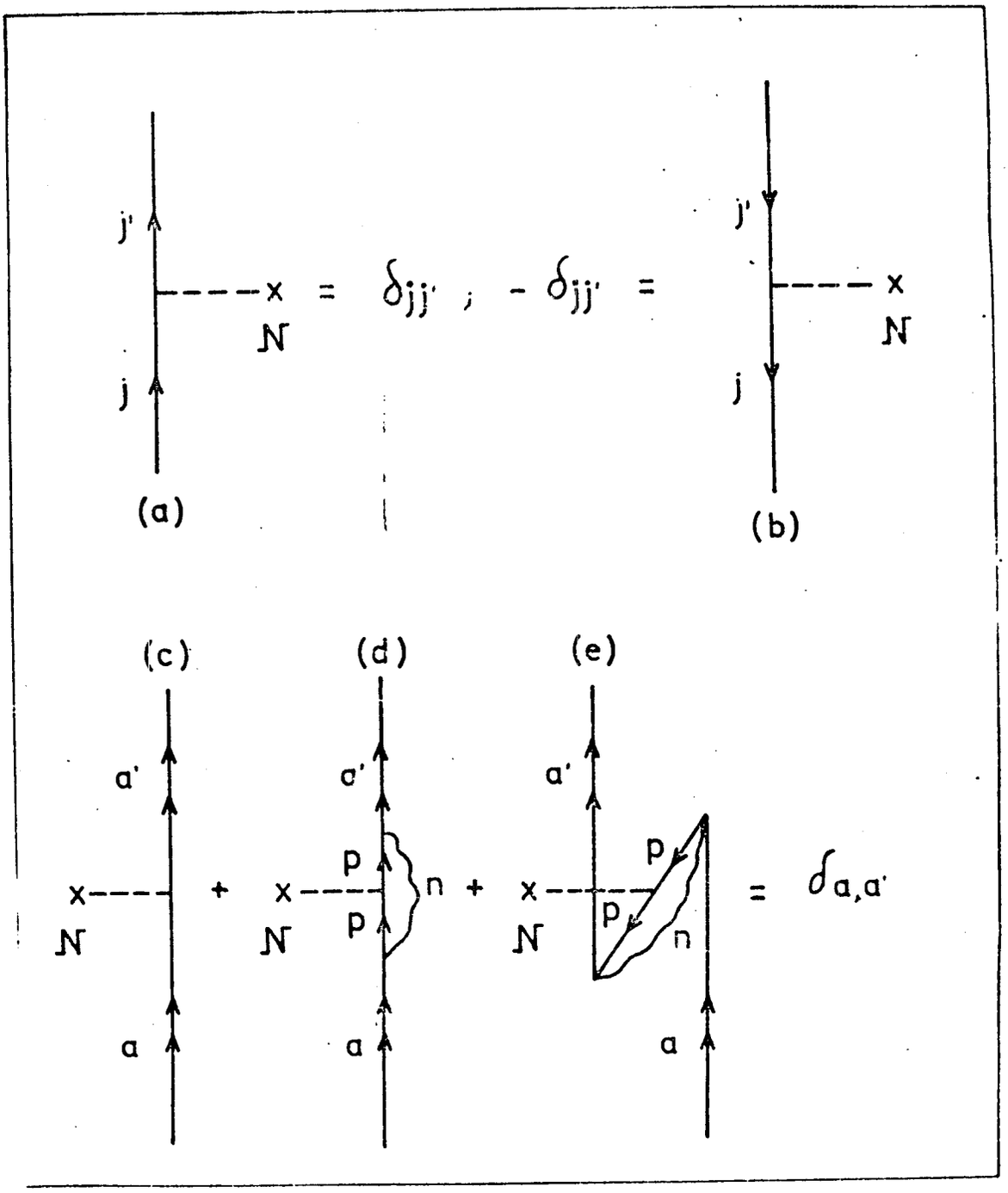


Fig. X-3

So far we have studied systems in which the elementary boson degrees of freedom are harmonic phonons. The rotations appear whenever the single-particle field violates a symmetry characteristic of the initial Hamiltonian. These symmetry-breaking fields are used whenever there is an imaginary root $\omega_n$ of RPA equations (II-13) or (III-10). In the particle-hole case, one includes in the fermion field a term of the form $-\chi Q_{coll} Q$, but where $Q_{coll} \tilde{=} Q_o \neq 0$ has a static non-vanishing value. For $\lambda = 2$, the corresponding eigenstates are given by the Nilsson wave functions (Ni 55). Because this description implies a priviliged orientation in space and, since the space is isotropic, rotational collective motion appears.

In the following, we treat the simpler problem of pairing rotations. In order to simplify the problem, we consider degenerate single-particle states with degeneracy

$$\Sigma_m = 2\Sigma_{m>o} = 2\Omega \tag{1}$$

The pairing monopole operators (III-8) and the fermion Hamiltonian[+] (III-7) reduce to

$$P^+ = \sum_{m>o} a_m^+ a_{\bar{m}}^+ \tag{2}$$

$$H_p = -\frac{1}{2} G (P^+P + PP^+) \tag{3}$$

Exact results obtained with a treatment with no symmetry breaking

It is easy to verify that the operators $P^+$, $P$ and

$$\Pi_{op} = \frac{1}{2}(N_{op} - \Omega) = \frac{1}{2}(\sum_m a_m^+ a_m - \Omega) \tag{4}$$

have the same commutation relations as the angular momentum operators $I_+$, $I_-$ and $I_z$. Thus, the eigensolutions of (3) carry $I = \frac{1}{2}(\Omega - \nu)$ and $I_z = \Pi$ as good quantum

---

+ This expression for $H_p$ differs from $H_p$ (eq.(III-7)) only through a trivial term proportional to the number of particles.

numbers. Here $\nu = 0,1,2,\ldots$ is called the seniority (Ra 43). The eigenvalues of $H_p$ and the matrix elements of $P^+$ are

$$E(\nu,\Pi) = -\frac{1}{4} G(\Omega-\nu)\ (\Omega+2-\nu) + G\Pi^2 \qquad (5)$$

$$< \nu'\Pi' |P^+| \nu\Pi > = \delta_{\nu\nu'}\, \delta_{\Pi'\Pi+1}\, \frac{1}{2}\ (\Omega-2\Pi-\nu)^{1/2}\ (\Omega+2\Pi+2-\nu)^{1/2} \qquad (6)$$

States with the same seniority are related by the two-dimensional rotational law $\Pi^2/2\mathcal{J}$ ($\mathcal{J} = (2G)^{-1}$ = moment of inertia ). The matrix elements of $P^+$ are fairly constant within a rotational band (at least if $\nu,\Pi \ll \Omega$) and vanish between two different bands (c.f. fig. XI-1).

Many nuclei display the qualitative characteristics implied by this coupling scheme. Fig. XI -2 shows the behavior of the Sn isotopes as an example.

Treatment with symmetry breaking terms

Similarly to the procedure outlined for the Nilsson's wave functions, the fermion states are defined through the deformed Hamiltonian

$$H'_p = -G<0|P|0>\ (P^+ + P) \qquad (7)$$

where the phase of $<0|P|0>$ has been chosen so that this expectation value is real. The system rotates in this phase space, and the orientations are labelled by the gauge angle $\phi$. The conjugate variable is the number of pairs of particles $\Pi$.

The deformed Hamiltonian $H'_p$ is diagonal in the single-fermion basis (Bo 58), (Va 58).

$$\alpha^+_m = 2^{-1/2}\ (a^+_m - a^+_{\bar{m}})$$
$$\alpha^+_{\bar{m}} = 2^{-1/2}\ (a^+_{\bar{m}} + a^+_m) \qquad m > 0 \qquad (8)$$

By means of the inverse transformation we express the pairing Hamiltonian (3) in terms of quasi-particles $\alpha^+_m$

$$
\begin{aligned}
H_p &= H_o\, H_{11} + H_{res} \\
H_o &= \frac{1}{4}\, G\, \Omega\, (\Omega+1) \\
H_{11} &= \frac{1}{2}\, G\, \Omega\, n_{op} \\
H_{res} &= \frac{1}{4}\, X G\, [p^+ p^+ + pp - 2p^+ p - n_{op}(n_{op} - 1)]
\end{aligned}
\tag{9}
$$

where

$$
n_{op} = \sum_m \alpha^+_m \alpha_m \quad ; \quad p^+ = \sum_{m>o} \alpha^+_m \alpha^+_{\bar{m}} \tag{10}
$$

It makes sense to work in the basis of independent quasi-particles (i.e., eigenfunctions of $H_o + H_{11}$) and to treat the residual interaction in perturbation theory. Therefore, we have introduced the small parameter X. Perturbation theory implies an expansion around $X=0$. Here we have the requirement that the expansion converges for $X=1$.

A straightforward application of Rayleigh-Schrödinger perturbation theory to (9) yields, for the ground state energy

$$
\begin{aligned}
E(gs) = & -\frac{1}{4}\, G\Omega^2 \\
& + G\Omega\left(\frac{1}{4} + \frac{X^2}{16} + \frac{X^3}{32} + \frac{5X^4}{256} + \frac{7X^5}{512} + \frac{21X^6}{2048} + \ldots\right) \\
& + G\left(-\frac{X^2}{16} + \frac{X^3}{32} + \frac{X^4}{64} + \frac{5X^5}{512} + \frac{7X^6}{1024} + \ldots\right) + G\Omega.O(\Omega^{-2})
\end{aligned}
\tag{12}
$$

We notice that the terms proportional to $G\Omega$ and G are, respectively, the power series expansion of

$$
-\frac{1}{4}\, G\Omega\left[3 - X - 2(1-X)^{1/2}\right]_{X\to 1} \to -\frac{1}{2}\, G\Omega \tag{14}
$$

$$
\frac{1}{16}\, G\left[4X - 3X^2 - 4X\,(1-X)^{1/2}\right]_{X\to 1} \to \frac{1}{16}\, G \tag{15}
$$

Therefore, the exact gs energy (eq. (5) with $\Pi=0$) is reproduced by the perturbation calculation to order $G\Omega$. The non-vanishing coefficient of the term proportional to G does not correspond to the exact result and is a consequence of the lack of convergence which is analytically discussed in the Appendix.

Let us now apply the NFT rules to the Hamiltonian (9). The phonon creation

operators are defined through

$$\Gamma^+ = Z\gamma^+ - Y\gamma \qquad \gamma^+ = \Omega^{-1/2}\, p^+ \tag{16}$$

The linearization condition $[H'_p, \Gamma^+] = \omega\Gamma^+$ yields

$$\begin{aligned} \omega &= G\Omega\ (1 - X)^{1/2} \\ Z &= \frac{1}{2}\left[(\omega/G\Omega)^{1/2} + (G\Omega/\omega)^{1/2}\right] \\ Y &= \frac{1}{2}\left[(\omega/G\Omega)^{1/2} - (G\Omega/\omega)^{1/2}\right] \end{aligned} \tag{17}$$

The ground state energy contribution due to the RPA is (see, for instance (Be 76a))

$$E_{RPA} = \frac{1}{2}\,\omega - \frac{1}{2}\,G(1-X/2) \xrightarrow{X\to 1} -\frac{1}{4}\,G\Omega \tag{18}$$

Therefore, the constant term $H_o$ plus the RPA contribution yields the exact energy of the lowest state (eq. (5)).

The particle-phonon vertices are given by the interaction term

$$\begin{aligned} H_{pv} &= -\Lambda\,(\Gamma - \Gamma^+)\,(p^+ - p) \\ \Lambda &= \frac{1}{2}\,G\Omega^{1/2}/(1-X)^{1/4} \end{aligned} \tag{19}$$

In spite of the fact that the coupling vertices diverge as $X\to 1$, the sum of all diagrammatic $\Omega^{-1}$ contributions is finite and is exactly given by (15). Thus, the NFT treatment reproduces the incorrect result of the perturbative fermion treatment.

Although we have only demonstrated the lack of convergence of the perturbative treatment of the residual Hamiltonian for the simplest of the deformed fields, it is likely that this feature is quite general. It is plausible that these problems arise because there are excited states in the intrinsic system which correspond to a different orientation of the system (i.e., spurious states). This fact would suggest that the problem may only be solved through a careful consideration of the constraints implicit in an intrinsic system. Powerful techniques have recently been introduced in quantum field theory in order to treat these problems (Di 64), (Fa 69), (Ha 76). The problem, however, appears to be

more complicated in nuclear physics, since here one must eliminate a complicate combination of the (original) fermion fields, and not an elementary boson field. To carry out this program represents a major challenge, and certainly a rewarding one: its importance lies not only on the relevance of the description of the rotational spectrum in nuclear physics, but also on the unification that it would imply in the common understanding of the different branches of physics.

Appendix

Since $p^+$,p and $\frac{1}{2}(n_{op}-\Omega)$ also obey SU2 commutation relations, it is easy to recast $H_p$ as

$$H_p = H_o - \frac{1}{2} G\Omega X^2 + G\Omega(1-X)(I_z+\Omega/2) + GxI_x^2 \qquad (20)$$

for the $I=\Omega/2,(v=0)$ representation. If X=1, the Hamiltonian (20) yields the eigenvalues (5), since

$$\Pi_{op} = \frac{1}{2}(p+p^+) = I_x \qquad (21)$$

Note however that the eigenfunctions of the number of pairs of particles $\Pi_{op}$ imply a large mixture of eigenstates of the number of quasi-particles $n_{op}$ (or of $I_z$).

The matrix corresponding to $H_p$ in the representation characterized by $I_z$ is reduced to two real tridiagonal matrices corresponding to an even or odd number of pairs of quasi-particles, respectively. The corresponding eigenvalues E are (branches of) analytical functions of X with only algebraic singularities (Sc 73). An exceptional point $X_o$ in the complex plane X is defined by the condition that for $X=X_o$ two eigenvalues coincide. These exceptional points are first order branch points of the two coinciding eigenvalues. The radius of convergence of the series expansion is smaller than the smallest value $|X_o|$.

We investigate the position of the exceptional points in two simple cases, namely I = 1 and I = 2.

---

+ I am grateful to A.Jackson for advice on the subject of this Appendix.

I=1 case. The matrix of order two

$$\begin{pmatrix} -\Omega(1-X) + \frac{1}{2}X & \frac{1}{2}X \\ \frac{1}{2}X & \Omega(1-X) + \frac{1}{2}X \end{pmatrix} \tag{22}$$

has eigenvalues

$$E = \frac{1}{2}X \pm \left[\Omega^2(1-X)^2 + X^2/4\right]^{1/2} \tag{23}$$

The exceptional points are located at the values for which the discriminant vanishes. Thus,

$$X_o = (1 \pm i/2\Omega)^{-1}$$
$$|X_o| = (1+1/4\Omega^2)^{-1} < 1 \tag{24}$$

I=2 case. For the matrix

$$\begin{pmatrix} -2\Omega(1-X) + X & \sqrt{\frac{3}{2}}X & 0 \\ \sqrt{\frac{3}{2}}X & 3X & \sqrt{\frac{3}{2}}X \\ 0 & \sqrt{\frac{3}{2}}X & 2\Omega(1-X)+X \end{pmatrix} \tag{25}$$

the vanishing of the discriminant requires

$$16\Omega^6(1-X)^6 + 4\Omega^4(1-X)^4X^2 + 103\Omega^2(1-X)^2X^4 + 9X^6 = 0 \tag{26}$$

For any value of $\Omega$, there are two roots on the upper half plane with $|X_o| < |$.

Although in these examples the relation $I=\Omega/2$ has been relaxed, the fact that $|X_o| <|$ for both I=1 and I=2 suggests that an expansion in powers of X cannot converge at the point X=1.

Figure Captions

Fig. XI-1: The spectrum of a pairing force for even systems with $\Pi>0$ and degeneracy $\Omega = 8$ (Be 77c). Each state is labelled by the quantum numbers $(\nu,\Pi)$. The transfer matrix elements are given within square brackets. They are normalized with respect to the matrix element $\langle \nu=0,\Pi=1 \,|P^+|\, \nu = 0,\ \Pi=0\rangle = 4.4$.

Fig. XI-2: Experimental energies of the $J^\pi = 0^+$ states of the even Sn-isotopes (Be 77c). The heavy drawn lines represent the values of the expression $E = -B(Sn) - E_{exc} + 8.50\,N + 45.3$ (MeV), where the binding energies B(A) (in MeV) are taken from (Wa 71). The dotted line represents the parabola $0.10\,(A-65.4)^2$, which corresponds to a rotational energy parameter $(2\mathcal{I})^{-1}=0.040$ MeV. Also displayed is the excited pairing rotational band associated with the pairing vibrational mode. In all cases where more than one $J^\pi = 0^+$ state has been excited below 3 MeV in two-neutron transfer processes, the energy of the centroid is quoted, as well as the cross section $\sum_i \sigma(0_i^+)$, where $\sigma(0_i^+)$ is the relative cross section with respect to the ground state cross section. The numbers along the abcisa are the ground state (p,t) and (t,p) cross sections normalized to the $^{116}Sn \leftrightarrow {}^{118}Sn$(gs) cross section. The (t,p) and (p,t) data utilized in constructing this figure were taken from Refs. (Bj 68), (Bj 69), (Fl 70a) and (Fl 70b).

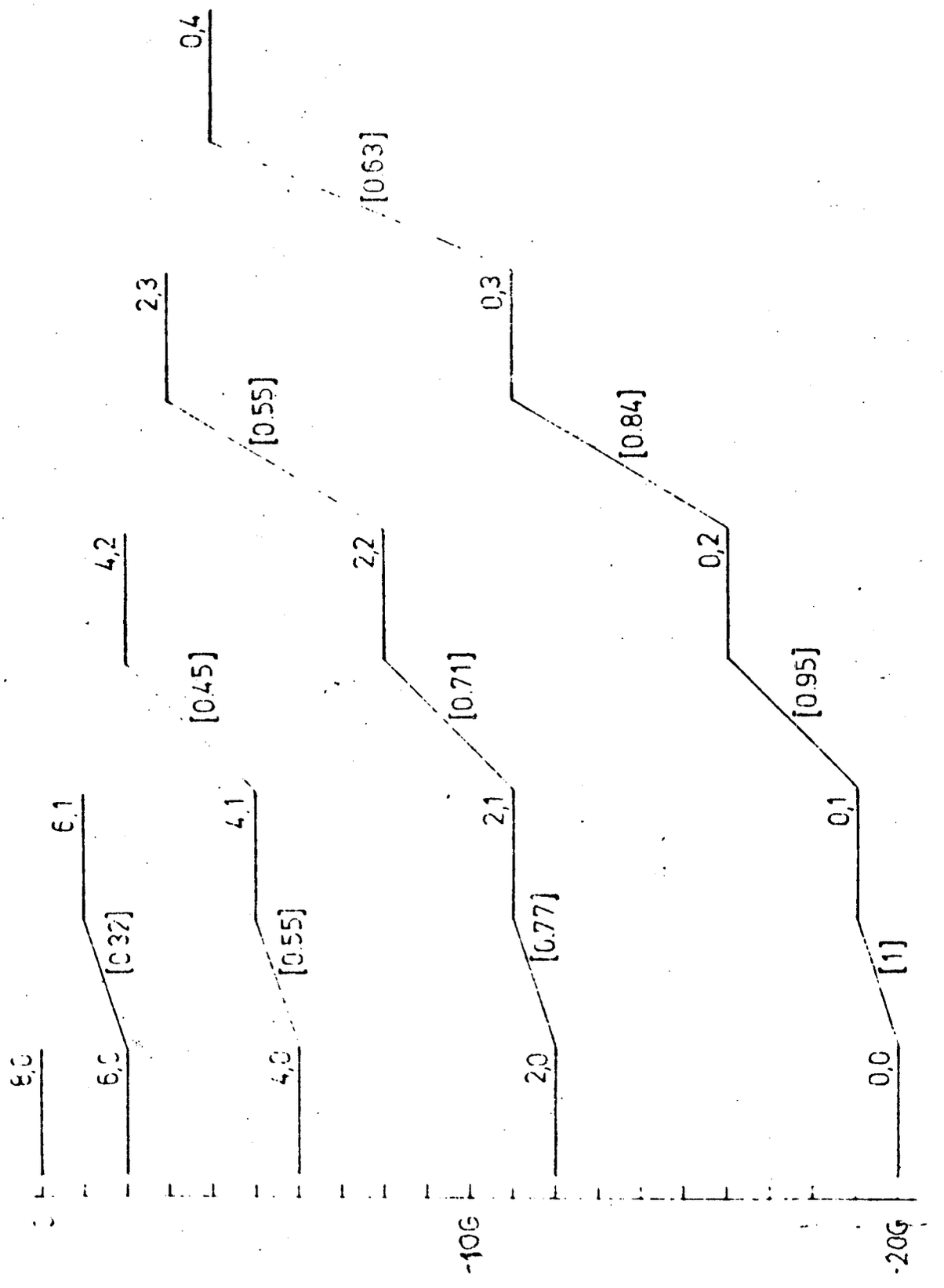
6,3
6,2
[0.32]
6,1
4,3
[0.55]
4,1
4,2
[0.45]
2,0
[0.77]
2,1
[0.71]
2,2
2,3
[0.55]
0,0
[1]
0,1
[0.95]
0,2
[0.84]
0,3
[0.63]
0,4
-10G
-20G

Fig. XI-1

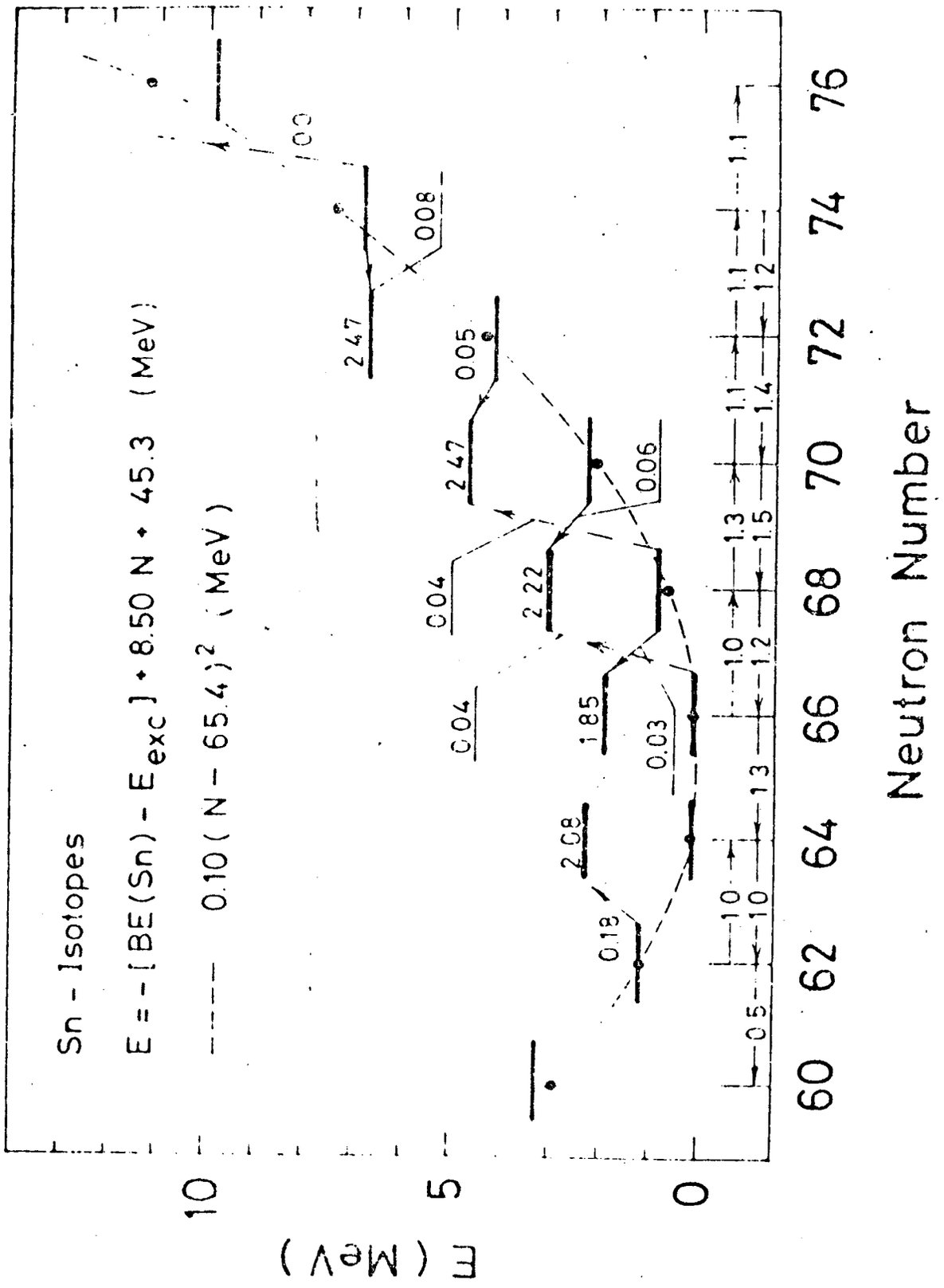
Sn - Isotopes
E = -[BE(Sn) - E_exc] + 8.50 N + 45.3 (MeV)
---- 0.10 ( N - 65.4 )^2 (MeV)
E (MeV)
10
5
0
60
62
64
66
68
70
72
74
76
Neutron Number
2.47
0.08
2.47
0.05
0.04
2.22
0.06
0.04
1.85
0.03
2.08
0.18
1.1
1.1
1.2
1.1
1.4
1.3
1.5
1.0
1.2
1.3
1.0
1.0
0.5

Fig. XI-2

I wish to express my gratirude to P.Mello for the opportunity of giving these lectures at the Escuela Latinoamericana de Física, which has enabled we to present recent advances on the coupling between the nuclear elementary degrees of freedom. Many years of interaction with the Copenhagen group, specially with A.Bohr, F.Bortignon, R.Broglia and B.Mottelson, have been essential for this review. A large fraction of the nuclear field theory has been developed in close colaboration with G.G.Dussel, R.Perazzo and H.Sofia in Buenos Aires and with O.Civitarese and R.Liotta both in Copenhagen and Buenos Aires. Stimulating discussions with O.Dragún, E.Maqueda,S.Reich and M.Saraceno are also gratefully acknowledged.

# REFERENCES


Ba 72 P.Barnes, E.Romberg, C.Ellegaard, R.Casten, O.Hansen, J.Mulligan, R.A. Broglia and R.Liotta, Nucl. Phys. A195, 146

Be 66 D.R.Bes and R.A.Broglia, Nucl. Phys. 80, 289

Be 69 D.R.Bes and R.A.Sorensen, Adv. in Nucl. Phys. 2, 129

Be 71 D.R.Bes and R.A.Broglia, Phys. Rev. 3C, 2349

Be 74 D.R.Bes, G.G.Dussel, R.A.Broglia, R.Liotta and B.R.Mottelson, Phys. Letters 52B, 253

Be 75 D.R.Bes, R.A.Broglia and B.S.Nilsson, Phys. Reports 16c1, 1

Be 76a D.R.Bes, R.A.Broglia, G.G.Dussel, R.Liotta and H.M.Sofía, Nucl. Phys. A260, 1 ; A260, 27

Be 76b D.R.Bes, R.A.Broglia, G.G.Dussel, R.Liotta and R.Perazzo, Nucl. Phys. A260, 77

Be 77a D.R.Bes, G.G.Dussel and H.M.Sofía, American Journal of Phys. 45, 191

Be 77b D.R.Bes, G.G.Dussel, R.Perazzo and H.M.Sofia, Nucl. Phys.

Be 77c D.R.Bes and R.A.Broglia, Proc. of the LIX Course of the Intern. School of Phys. "Enrico Fermi", to be published.

Bj 68 J.H.Bjrregaard, O.Hansen, O.Nathan, L.Vistisen, R.Chapman and S.Hinds, Nucl. Phys. A110, 1

Bj 69 J.H.Bjrregaard, O.Hansen, O.Nathan, R.Chapman and S.Hinds, Nucl.Phys. A131, 481

Bo 52 A.Bohr, Mat Fys. Medd. Dan. Vid. Selsk. 26, Nº 14

Bo 53 A.Bohr and B.R.Mottelson, Mat. Fys. Medd. Dan. Vid. Selsk. 27 Nº 16

Bo 58 N.Bogoliubov, Soviet Phys. JETP 7, 41.

Bo 64 A.Bohr, Compt. Rend. du Congres Intern. de Physique Nucléaire, ed. P. Gugenberger, CNRS, Paris

Bo 75 A.Bohr and B.R.Mottelson, Nuclear Structure II. W.A.Benjamin, Inc., Reading, Mass.

Bo 77a P.F.Bortignon, R.A.Broglia, D.R.Bes and R.Liotta, Phys. Reports 30c4, 309

Bo 77b P.F.Bortignon, R.A.Broglia and D.R.Bes, communication to the International Conference on Nuclear Structure, Tokyo

Br 70 R.A.Broglia, J.S.Lilley, R.Perazzo and W.R.Phillips, Phys.Rev. C1, 1508

Br 72 G.E.Brown, Many-Body Problems. North Holland Publishing Co., Amsterdam

Br 73 R.A.Broglia, O.Hansen and C.Riedel, Adv. in Nucl. Phys. 6, 287

Br 74 R.A.Broglia, D.R.Bes and B.Nilsson, Phys. Lett. 50B, 213

Br 76 R.A.Broglia, B.R.Mottelson, D.R.Bes, R.Liotta and H.M.Sofia, Phys. Lett. 64B, 29

Di 64 P.A.M.Dirac, Belfer Graduate School of Science, Yeshiva University,N.York

El 71 C.Ellegaard, P.D.Barnes and E.R.Flynn, Nucl. Phys. A170, 209

Fa 67 L.Fadeev and V.Popov, Kiev Report available in English as NAL-Thy-57

Fl 70a E.R.Flynn, J.G.Beery and A.G.Blair, Nucl. Phys. A154, 225

Fl 70b D.G.Fleming, M.Blann, H.W.Fulbright and J.A.Robbins, Nucl. Phys. A157,1

Fl 72a E.R.Flynn, G.J.Igo and R.A.Broglia, Phys. Letters 41B, 397

Fl 72b E.R.Flynn, G.J.Igo, R.A.Broglia, J.Landowne, V.Paar and B.Nilsson, Nucl. Phys. A195, 97

Fl 74 E.R.Flynn, R.A.Broglia, R.Liotta and B.S.Nilsson, Nucl. Phys. A221, 509

Ha 66 J.C.Hafele and R.Woods, Phys. Letters 23B, 579

Ha 69 I.Hamamoto, Nucl.Phys. A126, 545

Ha 74 I.Hamamoto, Phys. Reports 10c2, 63

Ha 76 A.Hansen, T.Regge and C.Teitelboim, Academia Nazionale dei Lincei, Rome

Ha 77 I.Hamamoto, Proc. of the LIX Course of the Intern. School of Phys."Enrico Fermi", to be published

He 69 J.W.Herlet, D.G.Fleming, J.P.Schiffer and H.E.Gove, Phys. Rev. Letters 23, 488

Ig 71 G.J.Igo, P.D.Barnes and E.R.Flynn, Ann. Phys. 66, 60

Ki 63 L.S.Kisslinger and R.A.Sorensen, Rev. Mod. Phys. 35, 853

La 41 L.Landau, J.Phys. USSR 5, 71

La 73 W.A.Lanford and J.B.McGrory, Phys. Letters 45B, 238

Mi 67 A.B.Migdal, Theory of Finite Fermi Systems and Applications to Atomic Nuclei, Interscience, New York

Mo 68 B.R.Mottelson, J.Phys. Soc. Japan, Suppl. 24, 87

Mo 77 B.R.Mottelson, Proc. of the LIX Course of the Intern. School of Phys. "Enrico Fermi", to be published

Ni 55 S.G.Nilsson, Mat. Fys. Medd. Dan. Vid. Selsk. 29, N°16

No 64 P.Nozieres, Theory of Interacting Fermi Systems. W.A.Benjamin, Inc. New York

Ra 43 G.Racah, Phys. Rev. 63, 367

Ra 59 J.B.Raz, Phys. Rev. 114, 1116

Sc 73 T.H.Schucan and H.A.Weidenmuller,Annals of Phys. 76, 483

Un 71 J.Ungrin, R.M.Diamond, P.O.Tjom and B.Elbeck, Kong. Dan. Vid. Selsk. Mat. Fys. Medd. 38, N°9

Va 58 J.G.Valatin, Nuovo Cimento 7, 843

Wa 71 A.H.Wapstra and N.B.Gove, Nucl. Data Tabels 9, 265

Wi 77 B.H.Wildenthal, Proc. of the LIX Course of the Intern. School of Phys. "Enrico Fermi", to be published

Zi 68 J.F.Ziegler and G.A.Peterson, Phys. Rev. 165, 1337